

BaySize: Bayesian Sample Size Planning for Phase I Dose-Finding Trials

Xiaolei Lin¹, Jiaying Lyu², Shijie Yuan², Sue-Jane Wang³, Yuan Ji^{4,*}

¹ School of Data Science, Fudan University, Shanghai, China

² 1. Laiya Consulting, Inc., Shanghai, China

³ US Food and Drug Administration, Silver Spring USA.

⁴ Department of Public Health Sciences, The University of Chicago, Chicago, USA

* corresponding: koaeraser@gmail.com;

Abstract

We propose BaySize, a sample size calculator for phase I clinical trials using Bayesian models. BaySize applies the concept of effect size in dose finding, assuming the MTD is defined based on an equivalence interval. Leveraging a decision framework that involves composite hypotheses, BaySize utilizes two prior distributions, the fitting prior (for model fitting) and sampling prior (for data generation), to conduct sample size calculation under desirable statistical power. Look-up tables are generated to facilitate practical applications. To our knowledge, BaySize is the first sample size tool that can be applied to a broad range of phase I trial designs.

Keywords: Bayes factor; Bayesian hypothesis testing; Fitting prior; Power; Sampling prior; Type I error.

1 Introduction

The primary objective of a phase I dose-finding trial is to identify the maximum tolerated dose (MTD) of an experimental drug. MTD is typically defined as the highest dose where the probability of the dose limiting toxicity (DLT) is close to or no higher than the target toxicity rate p_T , say $p_T = 0.30$. During the course of a trial, patients are accrued sequentially in cohorts, and dose assignment to a cohort of patients is dependent upon observed toxicity outcomes of the previously treated cohorts. Over the past three decades, a large number of dose-finding approaches have been proposed, including, for example, the 3+3 design (Storer, 1989), the continual reassessment method (CRM) (O’Quigley et al., 1990), the escalation with overdose control (EWOC) design (Babb et al., 1998), the cumulative cohort (CCD) design (Ivanova et al., 2007), the Bayesian optimal interval (BOIN) design (Liu and Yuan, 2015), the modified toxicity probability interval (mTPI, mTPI-2) methods (Ji et al., 2010, Ji and Wang, 2013, Guo et al., 2017), and the i3+3 design (Liu et al., 2020).

The number of patients required to achieve the scientific goal of a clinical trial is a major task to be considered in a statistical design since investigators only possess limited amount of resources and time. Larger sample sizes increase

the power of achieving trial objectives but also increase trial cost and duration. Despite flourishing literature in novel dose-finding designs, only a limited number of methods has been proposed for sample size determination for phase I trial design.

For clinical trials in general, not necessarily Phase I trials, Bayesian sample size determination approaches are based on various performance metrics, including, for example, the average posterior variance criterion (APVC) (Wang and Gelfand, 2002), the average length criterion (ALC), the worst outcome criterion (Joseph et al., 1995, Joseph and Belisle, 1997, M'lan et al., 2006, M'lan et al., 2008), and Bayes factors (Weiss, 1997). Zohar and Chevret (2001) calculated the required number of patients by considering different stopping rules in the CRM design. Lin and Shih (2001) and Ivanova (2006) described sample size recommendations on the basis of the expected number of patients allocated to each dose among prespecified dose levels. Tighiouart and Rogatko (2012) estimated the sample size using the posterior standard deviation and the highest posterior density interval of the MTD in the EWOC design. Recently, Cheung (2013) presented a closed-form formula for sample size calculation, in which a nonparametric optimal design (O'Quigley et al., 2002) was exploited and the accuracy index of the CRM design was derived empirically. These approaches, however, are tailored for specific designs, such as CRM or EWOC.

In this paper, we propose a general decision framework for sample size determination based on Bayesian hierarchical modeling. We set up two composite hypotheses indicating the presence and location of the true MTD, and apply Bayesian decision rules to select one of the hypotheses. Sample size is therefore decided according to desirable statistical power. Specifically, BaySize defines a composite null hypothesis H_0 "none of the doses are the MTD" and a composite alternative hypothesis H_1 "one of the doses is the MTD", and powers dose-finding trials based on the power of a Bayesian decision using the Bayes factor (BF). In addition, the proposed BaySize framework incorporates two types of priors - the fitting prior for BF estimation and the sampling prior for trial data generation, in order to achieve robustness and avoid inflating Type I error rate (Li et al., 2000).

The remainder of the article is organized as follows. Section 2 illustrates the BaySize framework in details and provides a searching algorithm for the desired sample size. A trial example is given in Section 3. In Section 4, the performance of BaySize is evaluated via extensive simulation studies with sensitivity analyses. The paper closes with a brief discussion in Section 5.

2 The BaySize Framework

2.1 Bayesian Hypothesis Testing for Phase I Dose-Finding Trials

Recent interval-based dose-finding designs, such as BOIN, i3+3, mTPI-2 and SPCRM (Liu and Yuan, 2015, Guo et al., 2017, Liu et al., 2020, Clertant and O’Quigley, 2017) define MTD as a dose with a toxicity probability falling into the EI, where $EI = [p_T - \epsilon_1, p_T + \epsilon_2]$ uses two small fractions. Suppose a total of D dose levels are prespecified for a Phase I dose-finding trial. Consider two hypotheses:

$$H_0 : \text{none of the prespecified doses are MTD} \quad \text{v.s.} \quad H_1 : \text{one of the prespecified doses is MTD.}$$

Denote p_d the DLT probability of dose d , $d = 1, 2, \dots, D$. We consider two composite hypotheses regarding the presence and location of the true MTD.

$$H_0 : \forall d, p_d \notin [p_T - \epsilon_1, p_T + \epsilon_2] \quad \text{v.s.} \quad H_1 : \exists d, p_d \in (p_T - \epsilon_1, p_T + \epsilon_2). \tag{1}$$

We define $(\epsilon_1 + \epsilon_2)$ as the “effect size” of the design, which describes the desired precision in MTD identification. The EI can be easily elicited from physicians by asking them the lowest and highest percentages of patients who have DLTs among, say 100 patients treated at the MTD. The effect size quantifies the desired accuracy in MTD identification. The larger or smaller the value of $(\epsilon_1 + \epsilon_2)$, the less or more accurate the MTD is to be identified, respectively. Since effect size is defined through the specification of EI in the context of interval-based designs, we hereinafter use the mTPI-2 design (Guo et al., 2017) as an example to further elaborate the BaySize framework. A brief discussion of the trivial extension of BaySize to accommodate other dose-finding designs is provided at the end of the paper.

Let X_d be the number of patients with DLTs and N_d the total number of patients treated at dose d , respectively, for $d = 1, 2, \dots, D$. Denote $\mathbf{p} = (p_1, p_2, \dots, p_D)$ the vector of the unknown toxicity probability at the D doses and $\mathbf{Y} \equiv \{(X_d, N_d), d = 1, 2, \dots, D\}$ the observed trial data. Under Bayesian hypothesis testing, a prior distribution of \mathbf{p} is constructed under each of the two hypotheses, H_0 and H_1 , defined as $\pi_0^{(f)}(\mathbf{p}|H_0)$ and $\pi_1^{(f)}(\mathbf{p}|H_1)$, respectively. Here the superscript “ f ” implies that these are the priors used to fit the data. Therefore, we call $\pi_0^{(f)}(\mathbf{p}|H_0)$ and $\pi_1^{(f)}(\mathbf{p}|H_1)$ the “fitting priors”. Later we will introduce another pair of priors called “sampling priors”, which are assumed to be the generative model for the trial data. The use of fitting and sampling priors is originally proposed in (Li et al., 2000) for non-inferiority trials. Given a dose-finding design \mathcal{E} (say, the mTPI-2 design) and the vector of toxicity probability \mathbf{p} , trial data \mathbf{Y} are assumed to follow a sampling distribution $f(\mathbf{Y}|\mathbf{p}, \mathcal{E})$. For the ease of exposition, hereinafter we drop the dependence on \mathcal{E} in mathematical derivation unless otherwise stated. For example, we will write $f(\mathbf{Y}|\mathbf{p})$ instead of $f(\mathbf{Y}|\mathbf{p}, \mathcal{E})$. But keep in mind that the subsequent model development always assumes an underlying dose-finding design \mathcal{E} .

The Bayesian hypothesis testing is based on the Bayes Factor $B(\mathbf{Y})$, which is defined as

$$B(\mathbf{Y}) = \frac{f(\mathbf{Y}|H_0)}{f(\mathbf{Y}|H_1)} = \frac{\int f(\mathbf{Y}|\mathbf{p}) \cdot \pi_0^{(f)}(\mathbf{p}|H_0) d\mathbf{p}}{\int f(\mathbf{Y}|\mathbf{p}) \cdot \pi_1^{(f)}(\mathbf{p}|H_1) d\mathbf{p}} \quad (2)$$

Given a critical cutoff value BF_0 , the Bayesian test chooses H_1 if $B(\mathbf{Y}) < BF_0$, and H_0 otherwise.

2.2 Sample Size Determination

For a Type I error rate α and Type II error rate β , BaySize determines the trial sample size by seeking an integer n that satisfies

$$\begin{aligned} \xi_0(n) &\equiv Pr \left\{ B(\mathbf{Y}^{(n)}) < BF_0 | H_0 \right\} \leq \alpha \quad (\text{Type I error}), \quad \text{and} \\ \xi_1(n) &\equiv Pr \left\{ B(\mathbf{Y}^{(n)}) < BF_0 | H_1 \right\} \geq 1 - \beta \quad (\text{Power}), \end{aligned}$$

where $\mathbf{Y}^{(n)}$ denotes the trial data under a sample size n . The two probabilities $\xi_0(n)$ and $\xi_1(n)$ are evaluated under the marginal distribution $f(\mathbf{Y}^{(n)}|H_i)$ defined as

$$f(\mathbf{Y}^{(n)}|H_i) = \int f(\mathbf{Y}^{(n)}|\mathbf{p}) \cdot \pi_i^{(s)}(\mathbf{p}|H_i) d\mathbf{p}, \quad i = 0, 1, \quad (3)$$

where $\pi_i^{(s)}(\mathbf{p}|H_i)$ is the sampling prior that generates the observed trial data $\mathbf{Y}^{(n)}$. Also $f(\mathbf{Y}^{(n)}|H_i)$ is known to Bayesians as the prior predictive distribution. Therefore, by definition we have

$$\xi_0(n) = \iint \mathbf{1} \left\{ B(\mathbf{Y}^{(n)}) < BF_0 \right\} f(\mathbf{Y}^{(n)}|\mathbf{p}) \pi_0^{(s)}(\mathbf{p}|H_0) d\mathbf{p} d\mathbf{Y}^{(n)}, \quad \text{and} \quad (4)$$

$$\xi_1(n) = \iint \mathbf{1} \left\{ B(\mathbf{Y}^{(n)}) < BF_0 \right\} f(\mathbf{Y}^{(n)}|\mathbf{p}) \pi_1^{(s)}(\mathbf{p}|H_1) d\mathbf{p} d\mathbf{Y}^{(n)} \quad (5)$$

where $\mathbf{1}\{\cdot\}$ is the indicator function that takes values 0 or 1. For sample size determination, the sampling priors $\pi^{(s)}$ and fitting priors $\pi^{(f)}$ should be different in order to avoid inflating the Type I error rate (Li et al., 2000). More details about both priors are provided in Sections 2.3 and 2.4. Since sample size determination must be done before the trial starts, the trial data $\mathbf{Y}^{(n)}$ has not yet been observed and is assumed to be random. Therefore, the Bayes Factor $B(\mathbf{Y}^{(n)})$ and the decision rule $\{B(\mathbf{Y}^{(n)}) < BF_0\}$, which are functions of the trial data $\mathbf{Y}^{(n)}$, are also random.

For a pre-determined Type I error rate α and power $(1 - \beta)$, BaySize determines the sample size by calculating

$$\boxed{n^* = \min\{\text{integer } n : \xi_0(n) \leq \alpha \text{ and } \xi_1(n) \geq 1 - \beta\}} \quad (6)$$

The main question is how to calculate n^* , which will be explained in the remainder of Section 2.

2.3 The Fitting Prior $\pi_0^{(f)}$ and $\pi_1^{(f)}$

Both the fitting and sampling priors must be specified in order to calculate $B(\mathbf{Y}^{(n)})$ and evaluate $\xi_0(n)$ and $\xi_1(n)$. We adopt the construction of the fitting priors $\pi^{(f)}(\mathbf{p} | H_0)$ and $\pi_1^{(f)}(\mathbf{p} | H_1)$ in the semi-parametric CRM model (SPCRM) by Clertant and O'Quigley (2017).

Under H_1 , the model space in SPCRM is partitioned by D submodels that provide the exact true MTD locations, given by

$$\begin{aligned} M_{11} : & \quad p_1 \in (p_T - \epsilon_1, p_T + \epsilon_2), \quad \text{and} \quad \forall d \neq 1, p_d \notin (p_T - \epsilon_1, p_T + \epsilon_2); \\ M_{12} : & \quad p_2 \in (p_T - \epsilon_1, p_T + \epsilon_2), \quad \text{and} \quad \forall d \neq 2, p_d \notin (p_T - \epsilon_1, p_T + \epsilon_2); \\ & \quad \dots \\ M_{1D} : & \quad p_D \in (p_T - \epsilon_1, p_T + \epsilon_2), \quad \text{and} \quad \forall d \neq D, p_d \notin (p_T - \epsilon_1, p_T + \epsilon_2). \end{aligned}$$

It is trivial that $H_1 = \bigcup_{d=1}^D M_{1d}$, since each submodel M_{1d} specifies one and only one dose level d as the true MTD. For example, submodel M_{11} states that only the first dose is in the equivalence interval and hence is the only true MTD. Given each submodel, the fitting prior can be easily specified according to Clertant and O'Quigley (2017). Specifically, conditional on model M_{1d} , the fitting prior $\pi_{1d}^{(f)}(\mathbf{p} | M_{1d})$ takes the form of a product of the independent truncated beta distribution, given by

$$\begin{aligned} \pi_{1d}^{(f)}(\mathbf{p} | M_{1d}) \propto & \quad \left[\prod_{k=1}^{d-1} \mathcal{B}_{LI} \{cq_k^{1d} + 1, c(1 - q_k^{1d}) + 1\} \right] \cdot \mathbb{I}(d > 1) \times \\ & \quad \mathcal{B}_{EI} \{cq_d^{1d} + 1, c(1 - q_d^{1d}) + 1\} \times \left[\prod_{k=d+1}^D \mathcal{B}_{HI} \{cq_k^{1d} + 1, c(1 - q_k^{1d}) + 1\} \right] \cdot \mathbb{I}(d < D), \quad (7) \end{aligned}$$

where \mathcal{B}_{LI} , \mathcal{B}_{EI} and \mathcal{B}_{HI} denote the truncated beta distributions on the lower interval (LI) $(0, p_T - \epsilon_1)$, the equivalence interval (EI) $[p_T - \epsilon_1, p_T + \epsilon_2]$ and the higher interval (HI) $(p_T + \epsilon_2, 1)$, respectively, $c \geq 0$ is a dispersion parameter, and q_k^{1d} is the mode of the truncated prior for the k th dose under equation (7). Let $\mathbf{q}^{1d} = (q_1^{1d}, \dots, q_D^{1d}) \in [0, 1]^D$ be the vector of the modes. A simple specification of \mathbf{q}^{1d} is provided in Appendix D.1 extending the idea in (Clertant and O'Quigley, 2017).

Similarly, under H_0 , the model space is partitioned into submodels as follows:

$$\begin{aligned}
 M_{00} &: \quad \forall d, p_d \in (p_T + \epsilon_2, 1); \\
 M_{01} &: \quad p_1 \in (0, p_T - \epsilon_1) \quad \text{and} \quad \forall d > 1, p_d \in (p_T + \epsilon_2, 1); \\
 M_{02} &: \quad \forall d \leq 2, p_d \in (0, p_T - \epsilon_1) \quad \text{and} \quad \forall d > 2, p_d \in (p_T + \epsilon_2, 1); \\
 &\dots \\
 M_{0,D-1} &: \quad \forall d \leq D-1, p_d \in (0, p_T - \epsilon_1), \quad \text{and} \quad p_D \in (p_T + \epsilon_2, 1); \\
 M_{0D} &: \quad \forall d, p_d \in (0, p_T - \epsilon_1).
 \end{aligned}$$

Each submodel corresponds to a subspace where none of the D doses are the true MTD. Specifically, the first model M_{00} indicates that all the doses are higher than the true MTD, the last model (M_{0D}) indicates that all the doses are lower than the true MTD, and the remaining models in between imply that the true MTD is sandwiched by two adjacent doses. Conditional on model M_{0d} , the fitting prior is given by

$$\pi_{0d}^{(f)}(\mathbf{p} | M_{0d}) \propto \left[\prod_{k=1}^d \mathcal{B}_{LI} \{cq_k^{0d} + 1, c(1 - q_k^{0d}) + 1\} \right] \cdot \mathbb{I}(d > 0) \times \left[\prod_{k=d+1}^D \mathcal{B}_{HI} \{cq_k^{0d} + 1, c(1 - q_k^{0d}) + 1\} \right] \mathbb{I}(d < D). \quad (8)$$

where \mathcal{B}_{LI} , \mathcal{B}_{HI} , $q_{0d} = (q_0^{0d}, \dots, q_D^{0d})$ and c denote the truncated beta distributions on the lower and higher intervals, their corresponding mode vector, and dispersion parameter, respectively.

To calculate the Bayes factor in (2), the following hierarchical model is specified. Denote m as the model indicator, for $i = 0, 1$,

$$\begin{aligned}
 \mathbf{Y}^{(n)} | \mathbf{p}, \mathcal{E} &\sim f(\mathbf{Y}^{(n)} | \mathbf{p}, \mathcal{E}), \\
 \pi_{id}^{(f)}(\mathbf{p} | m = M_{id}) &\sim (7) \text{ or } (8), \quad i = 1, 2, \quad d = 1, \dots, D \\
 M_{id} | H_i &\sim \pi(M_{id} | H_i) \cdot \mathbb{I}\{M_{id} \in \mathcal{M}_i\}, \quad i = 1, 2, \quad d = 1, \dots, D \\
 Pr(H_i) &= \frac{1}{2}, \quad i = 1, 2
 \end{aligned}$$

where the sets $\mathcal{M}_1 = \{M_{11}, M_{12}, \dots, M_{1D}\}$ and $\mathcal{M}_0 = \{M_{00}, M_{01}, \dots, M_{0D}\}$ contain D and $(D + 1)$ models, respectively. Without loss of generality, $\pi(M_{id} | H_i)$ is assumed to be uniform among the models in \mathcal{M}_0 and \mathcal{M}_1 , i.e., each model in \mathcal{M}_0 (or \mathcal{M}_1) is weighted equally under H_0 (or H_1). However, other prior can be considered based on available information for the doses. For example, one may assume $Pr(m = M_{1d} | H_1)$ is small for $d = 1$. That is, it is unlikely that the lowest dose is the MTD due to the fact that the lowest dose in a practical dose-finding trial is usually below the therapeutic window for safety reasons. Note that under the above hierarchical model specification,

the fitting priors under H_0 and H_1 can be derived by integrating out m , i.e., $\pi_i^{(f)}(\mathbf{p}|H_i) = \sum_{M_{ij} \in \mathcal{M}_i} \pi_{id}^{(f)}(\mathbf{p}|m = M_{id}, H_i) Pr(m = M_{id}|H_i)$, for $i = 0, 1$.

2.4 The Sampling Prior $\pi_0^{(s)}$ and $\pi_1^{(s)}$

Box (6) requires the evaluation of $\xi_0(n)$ and $\xi_1(n)$, which will be conducted by numerical simulation. Specifically, $\mathbf{Y}^{(n)}$ will be generated from the prior predictive distribution involving the construction of priors. To avoid inflating the Type I error rate and overfitting, the BaySize generates trial data using the sampling priors $\pi_0^{(s)}(\mathbf{p} | H_0)$ under H_0 and $\pi_1^{(s)}(\mathbf{p} | H_1)$ under H_1 , which differ from the aforementioned fitting priors. In this section, we provide some examples for sampling prior specification.

In practice, a statistical design \mathcal{E} is typically evaluated by simulating trial data under various scenarios. True probabilities of the candidate doses are prespecified for each scenario. Let \mathbf{p}_1^* denote the prespecified toxicity probabilities among which only one of the toxicity probabilities falls in the EI (i.e., one of the dose levels can be considered as the MTD). For example, if $p_T = 0.3$, EI = $[0.2, 0.4]$, and $D = 5$, then \mathbf{p}_1^* may be set as $(0.05, 0.09, 0.12, 0.19, 0.25)$. One simple method is to set $\pi_1^{(s)}(\mathbf{p} | H_1)$ as the point mass at \mathbf{p}_1^* , given by

$$\pi_1^{(s)}(\mathbf{p}|H_1) = \mathbf{1}\{\mathbf{p} = \mathbf{p}_1^*\} \quad (9)$$

Different \mathbf{p}_1^* values yield different sample size calculation. For instance, when the target toxicity probability $p_T = 0.3$ and EI = $[0.2, 0.4]$ (i.e., $\epsilon_1 = \epsilon_2 = 0.1$), larger sample size is required for $\mathbf{p}_1^* = (0.05, 0.09, 0.12, 0.19, 0.25)$ compared with $\mathbf{p}_1^* = (0.01, 0.3, 0.5, 0.6, 0.7)$, because the MTD is easier to identify for the latter case $\mathbf{p}_1^* = (0.01, 0.3, 0.5, 0.6, 0.7)$. This is simply because escalation to dose level 2 in $\mathbf{p}_1^* = (0.01, 0.3, 0.5, 0.6, 0.7)$ would achieve the MTD while in the former case the trial will need to escalate all the way to dose level 3 or 4. In addition to p_T and effect size ($\epsilon_1 + \epsilon_2$), several other factors need to be considered in specifying $\pi_1^{(s)}(\mathbf{p} | H_1)$ as reflected in Figure 1: 1) relative MTD location in the dose range, denoted as d^* , 2) relative MTD location in the equivalence interval, λ_1 , 3) distance from the lower bound of the equivalence interval to the next lower dose below MTD, ρ_1 , and 4) distance from the upper bound of the equivalence interval to the next higher dose above MTD, ρ_2 . These factors will be thoroughly investigated in the simulation study later.

Under H_0 , we consider the following three cases for the sampling prior $\pi_0^{(s)}(\mathbf{p} | H_0)$:

(Case i) order statistics from the uniform distribution $\mathcal{U}(0, p_T - \epsilon_1)$, i.e., $\mathbf{p} = (p_{(1)}, p_{(2)}, \dots, p_{(D)})$, $p_d \sim \mathcal{U}(0, p_T - \epsilon_1)$, $d = 1, 2, \dots, D$;

(Case ii) uniform distribution with monotonicity across doses,

$$\text{i.e., } p_1 \sim \mathcal{U}(0, p_T - \epsilon_1), p_2 \sim \mathcal{U}(p_1, p_T - \epsilon_1), \dots, p_D \sim \mathcal{U}(p_{D-1}, p_T - \epsilon_1);$$

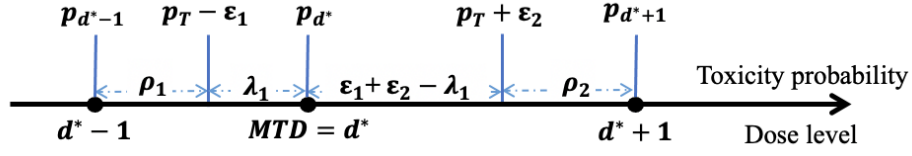


Figure 1: Factors that could potentially impact the configuration of p_1^* and the associated sampling prior in (9): the target toxicity rate (p_T), the effect size (ϵ_1 and ϵ_2), the MTD location in the dose range (i.e., the true MTD level, d^*), the MTD location in the EI (i.e., the distance from the lower boundary of EI $p_T - \epsilon_1$ to the MTD d^* , λ_1), and the distances from the lower / upper boundary of the EI to the next doses below / above the MTD (ρ_1 and ρ_2).



Figure 2: Three specific cases of the sampling priors under H_0 for $p_T = 0.3$, $\epsilon_1 = 0.05$ and $D = 5$.

(Case iii) point mass at $\mathbf{p} = (p_T - \epsilon_1, \dots, p_T - \epsilon_1)$, i.e., all doses have the same toxicity probability ($p_T - \epsilon_1$) (the worst case for sample size calculation).

See Figure 2 for an illustration. Note that for all three cases above, the toxicity probabilities are restricted in the subspace given by the null hypothesis H_0 , which is $\{p_d : p_d - p_T \leq \epsilon_1\}$, i.e., all dose levels are lower than $(p_T - \epsilon_1)$. In the case where all dose levels are higher than p_T , trials are likely to be terminated early by the safety rules adopted in many designs, such as the mTPI-2 design (Guo et al., 2017). For example, if $Pr(p_1 > p_T | data) > 0.95$, trial will be terminated early before reaching the sample size. Therefore, this case is not considered in specifying $\pi_0^{(s)}$.

2.5 Algorithm to Determine Sample Size

We develop Algorithm 1 to determine the optimal sample size n^* in Box (6) based on a numerical procedure. Given the target toxicity rate p_T , effect size ($\epsilon_1 + \epsilon_2$), Type I error rate α , Type II error rate β , and an upper bound for the maximum sample size n_U , the algorithm is initialized at n_U and then seeks an optimal sample size $n^* \leq n_U$ iteratively. During the j -th iteration (assuming the current sample size is n_j), the algorithm takes two steps to identify the next

proposed sample size n_{j+1} . In the first step, B trials are simulated under the null hypothesis H_0 and the cut-off value BF_0 is calculated to control the prespecified type I error rate α . Specifically, denote $BF_{0,b} = BF_0(\mathbf{Y}_b^{(n_j)})$, where $\mathbf{Y}_b^{(n_j)}$ is the data of the b -th simulated trial under sample size n_j . Then BF_0 is chosen to be the α -th quantile of $p(BF(\mathbf{Y}^{(n_j)})|H_0)$, the prior predictive distribution of $BF(\mathbf{Y}^{(n_j)})$ under H_0 , denoted as $BF_{0,\alpha}$. Numerically, $BF_{0,\alpha} = BF_{0,(\lfloor B \cdot \alpha \rfloor)}$, where (\cdot) is the order statistic and $\lfloor \cdot \rfloor$ is the floor function. In words, $BF_{0,\alpha}$ is the α -th percentile of $\{BF_{0,b}; b = 1, \dots, B\}$. In the second step, trial data are simulated under the alternative hypothesis H_1 and the cut-off value BF_0 calculated from step 1 is used to calculate the power $\xi_1(n_j) = Pr(B(\mathbf{Y}^{(n_j)}) < BF_{0,\alpha} | H_1)$. Here $\xi_1(n_j)$ is approximated by simulating C trials under H_1 . If the power is above the prespecified threshold $(1 - \beta)$ (i.e., the current sample size n_j is too large), the algorithm updates the sample size n_{j+1} to be the smallest integer that is greater than $\frac{n_j + n_j^-}{2}$ (i.e., $\lceil (n_j + n_j^-)/2 \rceil$), where n_j^- is the more recent sample size below n_j ; if the power is below $(1 - \beta)$ (i.e., the current sample size n_j is too small), the next optimal sample size n_{j+1} is updated to be the smallest integer that is larger than $\frac{n_j^+ + n_j}{2}$ (i.e., $\lceil (n_j^+ + n_j)/2 \rceil$), where n_j^+ is the more recent sample size above n_j . The algorithm converges when $|n_{j+1} - n_j| < \epsilon$ for a given threshold ϵ and the final sample size is determined to be the last n_{j+1} .

Algorithm 1 BaySize Algorithm for Prespecified p_T , (ϵ_1, ϵ_2) , α and β

- 1: Step 0: Initialization
 - 2: Initialize the sample size at $n_1 = n_U$, where n_U is the prespecified upper bound
 - 3: for $n_j < n_U$, $j > 1$, do:
 - 4: Step I: Type I error (α) calibration
 - 5: for $b = 1$ to B (recommended $B=1000$)
 - 6: a: Generate $\mathbf{p}_b \sim \pi_0^{(s)}(\mathbf{p} | H_0)$
 - 7: b: Generate $\mathbf{Y}_b^{(n_j)} \sim f(\mathbf{Y} | \mathbf{p}_b)$
 - 8: c: Calculate $BF_{0,b} = BF_0(\mathbf{Y}_b^{(n_j)})$
 - 9: Denote $S_0 = \{BF_{0,1}, \dots, BF_{0,B}\}$ and $BF_{0,\alpha} = BF_{0,(\lfloor B \cdot \alpha \rfloor)}$ be the α th percentile of S_0 . Then $\hat{\xi}_0(n_j) = \frac{1}{B} \sum_{b=1}^B I_{\{BF_{0,b} \leq BF_{0,\alpha}\}} \leq \alpha$
 - 10: Step II: Power $(1 - \beta)$ verification
 - 11: for $c = 1$ to C (recommended $C=1000$)
 - 12: a: Generate $\mathbf{p}_c \sim \pi_1^{(s)}(\mathbf{p} | H_1)$
 - 13: b: Generate $\mathbf{Y}_c^{(n_j)} \sim f(\mathbf{Y} | \mathbf{p}_c)$
 - 14: c: Calculate $BF_{1,c} = BF_0(\mathbf{Y}_c^{(n_j)})$
 - 15: Denote $S_1 = \{BF_{0,1}, \dots, BF_{0,C}\}$. Then $\hat{\xi}_1(n_j) = \frac{1}{C} \sum_{c=1}^C I_{\{BF_{0,c} \leq BF_{0,\alpha}\}}$
 - 16: if $\hat{\xi}_1(n_j) > 1 - \beta$,
 - 17: $n_{j+1} = \lceil (n_j + n_j^-)/2 \rceil$, where n_j^- is the most recent sample size below n_j ;
 - 18: else if $\hat{\xi}_1(n_j) \leq 1 - \beta$,
 - 19: $n_{j+1} = \lceil (n_j^+ + n_j)/2 \rceil$, where n_j^+ is the most recent sample size above n_j ;
- 20: Step III: repeat Step I and II until $|n_{j+1} - n_j| < \epsilon$, where ϵ is a prespecified threshold.
- 21: Output: the final n_{j+1}
-

3 Look-Up Table

For practical trials, the sample size determination is often conducted before a trial begins and as a result the toxicity probabilities \mathbf{p}_1^* under H_1 is unknown. Table 1 calculates the power for each candidate sample size given a range of effect sizes and Type I error rates for $p_T = 0.3$. For instance, when the half effect size $\epsilon_1 = \epsilon_2 = 0.1$, Type I error rate is controlled at 30% and power no less than 80%, the minimum sample size needed is 60. Here the simulation-based

searching algorithm for the BaySize framework adopts five different scenarios for \mathbf{p}_1^* where in each scenario, the true MTD locates at a different dose level. In Table E.2 of Appendix E, we provide the sample size look-up table for $p_T = 0.2$.

Table 1: For each combination of the half effect size $\epsilon_1 = \epsilon_2$, Type I error rate α and candidate sample size, the range of the power $(1 - \beta)$ given $p_T = 0.3$ is calculated under five different scenarios of \mathbf{p}_1^* , where for each scenario, the true MTD locates at a different dose level as reflected in Figure A.2.

Half effect size	Type I error rate	Power min~max				
		n=30	n=45	n=60	n=75	n=90
0.05	0.05	0.11~0.20	0.09~0.17	0.09~0.18	0.10~0.19	0.12~0.21
	0.1	0.18~0.25	0.18~0.25	0.20~0.29	0.26~0.35	0.30~0.40
	0.2	0.34~0.45	0.38~0.45	0.47~0.53	0.53~0.57	0.60~0.63
	0.3	0.51~0.62	0.58~0.61	0.68~0.70	0.71~0.75	0.73~0.79
	0.4	0.63~0.68	0.71~0.77	0.76~0.82	0.79~0.85	0.79~0.87
	0.5	0.74~0.82	0.79~0.85	0.81~0.88	0.84~0.91	0.86~0.92
0.1	0.05	0.09~0.31	0.18~0.36	0.24~0.42	0.33~0.46	0.42~0.52
	0.1	0.23~0.49	0.37~0.53	0.43~0.57	0.52~0.60	0.62~0.67
	0.2	0.46~0.59	0.59~0.69	0.69~0.72	0.75~0.77	0.78~0.80
	0.3	0.61~0.71	0.73~0.77	0.80~0.85	0.81~0.88	0.85~0.92
	0.4	0.71~0.79	0.84~0.90	0.85~0.92	0.87~0.94	0.88~0.95
	0.5	0.82~0.91	0.86~0.93	0.89~0.96	0.90~0.97	0.90~0.97
0.15	0.05	0.24~0.59	0.40~0.62	0.51~0.67	0.60~0.71	0.67~0.75
	0.1	0.33~0.62	0.48~0.69	0.68~0.77	0.71~0.78	0.80~0.82
	0.2	0.58~0.77	0.73~0.80	0.86~0.90	0.84~0.86	0.87~0.90
	0.3	0.73~0.85	0.86~0.90	0.86~0.90	0.88~0.94	0.88~0.95
	0.4	0.75~0.85	0.88~0.95	0.90~0.96	0.90~0.97	0.90~0.97
	0.5	0.87~0.92	0.92~0.98	0.96~0.99	0.96~0.99	0.96~0.99
0.2	0.05	0.37~0.64	0.62~0.72	0.77~0.81	0.81~0.86	0.83~0.87
	0.1	0.67~0.79	0.80~0.83	0.84~0.86	0.85~0.88	0.87~0.91
	0.2	0.73~0.82	0.88~0.92	0.88~0.93	0.90~0.95	0.90~0.95
	0.3	0.90~0.96	0.90~0.96	0.91~0.97	0.91~0.97	0.91~0.98
	0.4	0.90~0.96	0.96~0.99	0.96~0.99	0.96~0.99	0.97~0.99
	0.5	0.91~0.98	0.96~0.99	0.96~0.99	0.97~0.99	0.97~0.99

4 Simulation Studies

4.1 Simulation Setup

Without loss of generality, we consider trials with the target toxicity rate $p_T = 0.3$ and the number of dose levels $D = 5$. Trials are simulated using the mTPI-2 design (Guo et al., 2017) with the first dose as the starting dose and a cohort size of 3. Type I error rate is controlled at various prespecified levels ranging between 0.05 and 0.50. Four values are considered for half effect size $\epsilon_1 = \epsilon_2 = (0.05, 0.10, 0.15, 0.20)$. For each effect size, five scenarios are considered for \mathbf{p}_1^* under H_1 where the true MTD corresponds to a different dose level. Specifically, for each scenario of \mathbf{p}_1^* , the toxicity probability of the true MTD is set to be p_T , i.e., the true MTD lies exactly in the middle of the EI with $p_{d^*} = p_T$, $p_{d^*-1} = p_T - \epsilon_1$ and $p_{d^*+1} = p_T + \epsilon_2$, where d^* is the true MTD. For the sampling prior

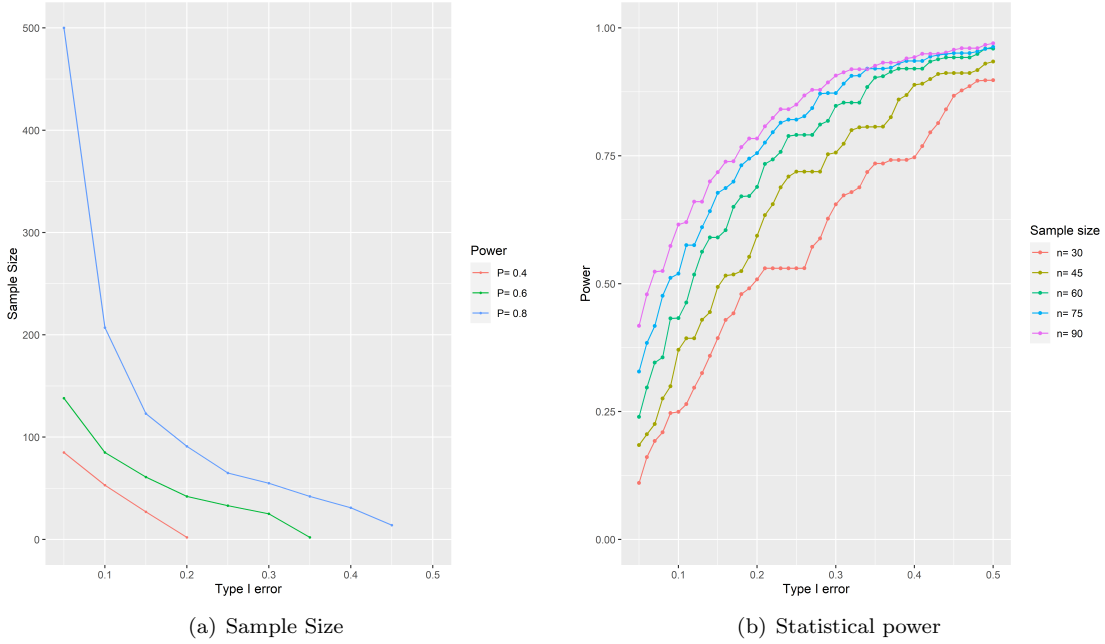


Figure 3: Sample size and statistical power calculated according to BaySize given $p_T = 0.3$, half effect size $\epsilon_1 = \epsilon_2 = 0.1$, $\mathbf{p}_1^* = (0.1, 0.2, 0.3, 0.4, 0.5)$ and Type I error rate controlled between 5% and 50%. (a) Sample size when statistical power equals 40%, 60% and 80%. (b) Statistical power when candidate sample size equals 30, 45, 60, 75 and 90.

$\pi_0^{(s)}(\mathbf{p} | H_0)$ under H_0 , we use the order statistics from the uniform distribution (Case (i) in Section 2.4). Finally, vague fitting priors are used for both H_0 and H_1 with $c = 0$ in equation (7) and (8). Two types of simulations are conducted. First, sample size is calculated according to Algorithm 1 for a range of Type I error rate and power. A practical consideration in trial design is to set the maximum sample size to be the multiple of dose levels. Therefore, in the second type of simulations, a set of candidate sample sizes are specified and statistical power is calculated for each combination of Type I error rate and candidate sample size. We set up scenarios with varying factors, such as the MTD location in the EI (λ_1), and the distance from the lower / upper bound of the EI to the adjacent doses (ρ_1 and ρ_2), as shown in Figure 1. Finally, sensitivity analyses are conducted to evaluate different specifications of the sampling prior $\pi_0^{(s)}(\mathbf{p} | H_0)$ and the fitting prior $\pi_1^{(f)}(\mathbf{p} | H_0)$ and $\pi_1^{(f)}(\mathbf{p} | H_1)$, e.g., different specifications of dispersion parameter c and mode vector \mathbf{q}^{1d} and \mathbf{q}^{2d} in equation (7) and (8).

4.2 Simulation Results

Figure 3(a) and 3(b) demonstrate the sample size and statistical power calculated by BaySize when power equals 40%, 60%, 80%, and candidate sample size equals 30, 45, 60, 75 and 90, for $p_T = 0.3$, half effect size $\epsilon_1 = \epsilon_2 = 0.1$, $\mathbf{p}_1^* = (0.1, 0.2, 0.3, 0.4, 0.5)$ and Type I error rate controlled between 5% and 50%

As expected, for fixed p_T , effect size ($\epsilon_1 + \epsilon_2$), \mathbf{p}_1^* and Type I error rate α , sample size increases with power, shown in Figure 3(a). For example, when Type I error rate is set at $\alpha = 0.15$, one needs to enroll 29, 65 and 123 subjects to

achieve 40%, 60% and 80% statistical power, respectively. Taking a different angle, for fixed p_T , effect size $(\epsilon_1 + \epsilon_2)$, \mathbf{p}_1^* and Type I error rate α , power increases with sample size, as is reflected in Figure 3(b). For example, when the Type I error rate $\alpha = 0.3$, statistical power increases from 65.50% to 75.64%, 84.77%, 87.25%, 90.70% as the sample size increases from 30 to 45, 60, 75, 90. An important observation from these results is that the gain of statistical power diminishes as sample size increases. In Figure 3(b), statistical power increases by 10.14%, 9.13%, 2.48% and 3.45% when the sample size increases every 15 units from 30 to 45, 60, 75 and 90. Full simulation results for the sample size and power calculation for each combination of the effect size and \mathbf{p}_1^* is shown in Figure A.1 and A.2 of Appendix A.

Next, we consider the effect of relative MTD location on the sample size and statistical power. As shown in Figure A.1 and A.2, the lower the true MTD location, the easier it is to be identified, and thus the smaller the sample size with fixed power, or the higher the power with fixed sample size. This is expected since dose finding usually starts at the lowest dose and the MTD is more difficult to reach in dose finding trials when it is located at a higher dose level. It should also be noticed that given an effect size $(\epsilon_1 + \epsilon_2)$ and sample size n , the gain of power depends on \mathbf{p}_1^* as well. For instance, consider $\epsilon_1 = \epsilon_2 = 0.1$ (the second row in Figure A.2) and sample size $n = 30$ (the red line in Figure A.2), power increases by 52.69% (from 30.56% to 83.25%) for $\mathbf{p}_1^* = (0.3, 0.4, 0.5, 0.6, 0.7)$, while 69.6% (from 12.28% to 81.88%) for $\mathbf{p}_1^* = (0.01, 0.05, 0.1, 0.2, 0.3)$. There are possibly two explanations. First, for $\mathbf{p}_1^* = (0.3, 0.4, 0.5, 0.6, 0.7)$ where the first dose is the true MTD and all doses above are overly toxic, the algorithm in mTPI-2 design basically allocates the most patients to the first two doses and almost no patients to the last three doses. While for $\mathbf{p}_1^* = (0.01, 0.05, 0.1, 0.2, 0.3)$ where all doses are safe and the last dose is considered as the true MTD, patients are allocated to all five doses and inference about the toxicity probability p_d is done at all dose levels, which facilitates the fast increasing of the power. Secondly, scenarios with $\mathbf{p}_1^* = (0.3, 0.4, 0.5, 0.6, 0.7)$ are more likely to be terminated by the safety rules in many designs such as mTPI-2, and as a result, the average number of patients enrolled and treated is fewer than the maximum sample sizes prespecified. This is particularly obvious from the sub-figure (row 2, column 1) in Figure A.2 that the power barely increases from $n = 75$ to $n = 90$.

Finally, if we compare each column in Figure A.1 and A.2 with the same \mathbf{p}_1^* and different effect sizes $(\epsilon_1 + \epsilon_2)$, it is easy to find that given a fixed power, fewer patients are needed for larger effect size, and given a fixed candidate sample size, higher power is achieved for larger effect size. This indicates that MTD is easier to be identified for larger effect sizes, possibly due to the reason that given $p_T = 0.3$, it is easier to distinguish the toxicity probability between 0.3 and 0.15 than between 0.3 and 0.25. In addition, for large effect size such as $\epsilon_1 = \epsilon_2 = 0.2$ (the last row in Figure A.1 and A.2), the power quickly reaches its plateau (close to 1) for all candidate sample sizes when α increases from 0.05 to 0.5. In other words, the power gain in the context of large effect sizes is limited compared with small effect sizes.

Simulation results for $p_T = 0.2$ are provided in Appendix B and similar patterns are observed. In addition, various

factors that could potentially affect the sample size determination (and power calculation) are thoroughly investigated and results are provided in Appendix C. In summary, C.4 and C.5 indicate that fewer patients are needed if the true MTD locates in the middle of the equivalence interval, while Figures C.6, C.7, C.8 and C.9 indicate that distances from the lower / upper bounds of the equivalence interval to the adjacent doses below / above the MTD has little impact on the sample size determination.

4.3 Sensitivity Analysis

The effects of different sampling priors $\pi_0^{(s)}(\mathbf{p} | H_0)$, dispersion parameters c and mode vectors (\mathbf{q}^{1d} and \mathbf{q}^{0d}) of the fitting priors are investigated through a series of sensitivity analyses. Results are provided in Appendix D.2. In brief, Figures D.10 indicates that the specification of $\pi_0^{(s)}(\mathbf{p} | H_0)$ has a large impact on the power calculation and thus on sample size determination. Given $p_T = 0.3$ and $\epsilon_1 = \epsilon_2 = 0.1$, for a fixed \mathbf{p}_1^* and α , order statistics from the uniform distribution (Case i in Section 2.4) always has the largest power for a given sample size n , and thus the smallest sample size given a prespecified power. This is because the doses generated from the order statistics sampling prior are more dispersed and further away from p_T , and as a result, it is easier to accept H_0 under the null. With a large calibrated BF_0 in step 1 of Algorithm 1, one would get a larger power for each n (and small n for each prespecified power level). Figure D.11 and D.12 indicate that given $p_T = 0.3$ and $\epsilon_1 = \epsilon_2 = 0.1$, the effect of fitting prior is overall small.

5 Discussion

In this paper, we propose a general Bayesian framework for sample size determination in Phase I dose-finding trials, through formal Bayesian decision making under two composite hypotheses. The performance of BaySize was evaluated via extensive simulation studies and results show that for a prespecified effect size and fitting / sampling priors, BaySize is able to control Type I error rate while achieving enough power. Note that the “power” in BaySize does not imply the correct selection of the true MTD, an objective of dose-finding designs rather than sample size calculation. What BaySize is concerned about is to empower the dose-finding trial so that when the true MTD is present, the pre-planned sample size will allow investigators to identify it with a sound statistical model and a design, such as the fitting prior and the mTPI-2 design proposed in this paper.

The BaySize approach can account for parameter uncertainties through prior specifications of the toxicity profiles. Specifically, for fitting priors in the Bayes Factor thresholding, the model space is augmented and divided into multiple sub-spaces in order to facilitate the prior construction; while for sampling priors in trial data generation, historical trial data or information about relevant trials can be incorporated for better specifications of the toxicity profiles. Besides, BaySize determines the minimum required sample size according to the prespecified Type I error

rate and power. Although the sample size determination relies on a simulation-based searching algorithm and does not have a closed form solution, the fast computing speed of modern computers makes this method easy to implement.

Although the development of BaySize is illustrated using the mTPI-2 design throughout this paper, it can be easily extended to other designs as well, such as CRM and BOIN. In making inferences about the toxicity profiles and conducting hypothesis testing, BaySize collects the number of DLTs and total number of patients allocated at each dose. While trial data are simulated under a specific design, the simulation process is generally separated from the MTD identification and thus sample size determination. Therefore, BaySize is generally applicable as long as the design algorithms can output the toxicity outcomes given a prespecified maximum sample size. Furthermore, BaySize can be extended to time-to-event designs, such as TITE-CRM, TITE-BOIN and POD-TPI, where patients accrual can be continued with late-on-set toxicities via time to event modeling (Cheung and Chappell, 2000, Yuan et al., 2018, Zhou et al., 2020). Finally, BaySize can be extended to also include efficacy outcomes, which is important for dosing scenarios with non-monotonic dose-response relationship.

References

- Barry E Storer. Design and analysis of phase i clinical trials. *Biometrics*, pages 925–937, 1989.
- John O’Quigley, Margaret Pepe, and Lloyd Fisher. Continual reassessment method: a practical design for phase 1 clinical trials in cancer. *Biometrics*, pages 33–48, 1990.
- James Babb, André Rogatko, and Shelemyahu Zacks. Cancer phase i clinical trials: efficient dose escalation with overdose control. *Statistics in medicine*, 17(10):1103–1120, 1998.
- Anastasia Ivanova, Nancy Flournoy, and Yeonseung Chung. Cumulative cohort design for dose-finding. *Journal of Statistical Planning and Inference*, 137(7):2316–2327, 2007.
- Suyu Liu and Ying Yuan. Bayesian optimal interval designs for phase i clinical trials. *Journal of the Royal Statistical Society: Series C (Applied Statistics)*, 64(3):507–523, 2015.
- Yuan Ji, Ping Liu, Yisheng Li, and B Nebiyu Bekele. A modified toxicity probability interval method for dose-finding trials. *Clinical Trials*, 7(6):653–663, 2010.
- Yuan Ji and Sue-Jane Wang. Modified toxicity probability interval design: a safer and more reliable method than the 3+ 3 design for practical phase i trials. *Journal of Clinical Oncology*, 31(14):1785–1791, 2013.
- Wentian Guo, Sue-Jane Wang, Shengjie Yang, Henry Lynn, and Yuan Ji. A bayesian interval dose-finding design addressing cockham’s razor: mtpi-2. *Contemporary clinical trials*, 58:23–33, 2017.
- M. Liu, S.J. Wang, and Y. Ji. The i3+3 design for phase i clinical trials. *Journal of Biopharmaceutic Statistics*, 30(2):294–304, 2020.
- Fei Wang and Alan E Gelfand. A simulation-based approach to bayesian sample size determination for performance under a given model and for separating models. *Statistical Science*, pages 193–208, 2002.
- Lawrence Joseph, David B Wolfson, and Roxane Du Berger. Sample size calculations for binomial proportions via highest posterior density intervals. *The Statistician*, pages 143–154, 1995.
- Lawrence Joseph and Patrick Belisle. Bayesian sample size determination for normal means and differences between normal means. *Journal of the Royal Statistical Society: Series D (The Statistician)*, 46(2):209–226, 1997.
- Cyr Emile M’Lan, Lawrence Joseph, and David B Wolfson. Bayesian sample size determination for case-control studies. *Journal of the American Statistical Association*, 101(474):760–772, 2006.
- Cyr E M’lan, Lawrence Joseph, David B Wolfson, et al. Bayesian sample size determination for binomial proportions. *Bayesian Analysis*, 3(2):269–296, 2008.
- Robert Weiss. Bayesian sample size calculations for hypothesis testing. *Journal of the Royal Statistical Society: Series D (The Statistician)*, 46(2):185–191, 1997.

- Sarah Zohar and Sylvie Chevret. The continual reassessment method: comparison of bayesian stopping rules for dose-ranging studies. *Statistics in medicine*, 20(19):2827–2843, 2001.
- Yong Lin and Weichung J Shih. Statistical properties of the traditional algorithm-based designs for phase i cancer clinical trials. *Biostatistics*, 2(2):203–215, 2001.
- Anastasia Ivanova. Escalation, group and a+ b designs for dose-finding trials. *Statistics in Medicine*, 25(21):3668–3678, 2006.
- Mourad Tighiouart and Andre Rogatko. Number of patients per cohort and sample size considerations using dose escalation with overdose control. *Journal of Probability and Statistics*, 2012, 2012.
- Ying Kuen Cheung. Sample size formulae for the bayesian continual reassessment method. *Clinical Trials*, 10(6): 852–861, 2013.
- John O’Quigley, Xavier Paoletti, and Jean Maccario. Non-parametric optimal design in dose finding studies. *Biostatistics*, 3(1):51–56, 2002.
- Wenqing Li, Ming-Hui Chen, Xiaojing Wang, and Dipak K Dey. Bayesian design of non-inferiority clinical trials via the bayes factor. *Statistics in Biosciences*, pages 1–21, 2000.
- Matthieu Clertant and John O’Quigley. Semiparametric dose finding methods. *Journal of the Royal Statistical Society: Series B (Statistical Methodology)*, 79(5):1487–1508, 2017.
- Ying Kuen Cheung and Rick Chappell. Sequential designs for phase i clinical trials with late-onset toxicities. *Biometrics*, 56:1177–1182, 2000.
- Ying Yuan, Ruitao Lin, Daniel Li, Lei Nie, and Katherine Warren. Time-to-event bayesian optimal interval design to accelerate phase i trials. *Clinical Cancer Research*, 24(20):4921–4930, 2018.
- Tianjian Zhou, Wentian Guo, and Yuan Ji. Pod-tpi: Probability-of-decision toxicity probability interval design to accelerate phase i trials. *Statistics in bioscience*, 12:124–145, 2020.

Appendices

Appendix A Full Simulation Results

Full simulation results comparing the sample size calculation for each combination of half effect size and p_1^* are summarized in Figure A.1.

Full simulation results comparing the statistical power for each combination of half effect size and p_1^* are summarized in Figure A.2.

Appendix B Simulation for $p_T = 0.2$

Simulation studies are conducted for $p_T = 0.2$. Results are summarized in Figure B.3.

Appendix C Other Factors that Could Impact the Sample Size Determination

Simulation studies are conducted to investigate the effect of MTD location in the EI (λ_1), and the distances from the lower / upper boundary of the EI to the next dose below / above the MTD (ρ_1 and ρ_2). Trials are simulated under half effect size $\epsilon_1 = \epsilon_2 = 0.1$ and $\epsilon_1 = \epsilon_2 = 0.15$, respectively. Results are shown in Figures C.4, C.5, C.6, C.7, C.8 and C.9.

Overall, ρ_1 and ρ_2 have limited impact on the statistical power and sample size determination, according to Figure C.6, C.7, C.8 and C.9. Figures C.4 and C.5 indicate that, for scenarios where the first or the last dose is the true MTD, larger power (given the candidate sample size) or smaller sample size (given the prespecified power rate) is observed when the true MTD locates toward the middle of the EI, i.e., when λ_1 moves further away from 0.

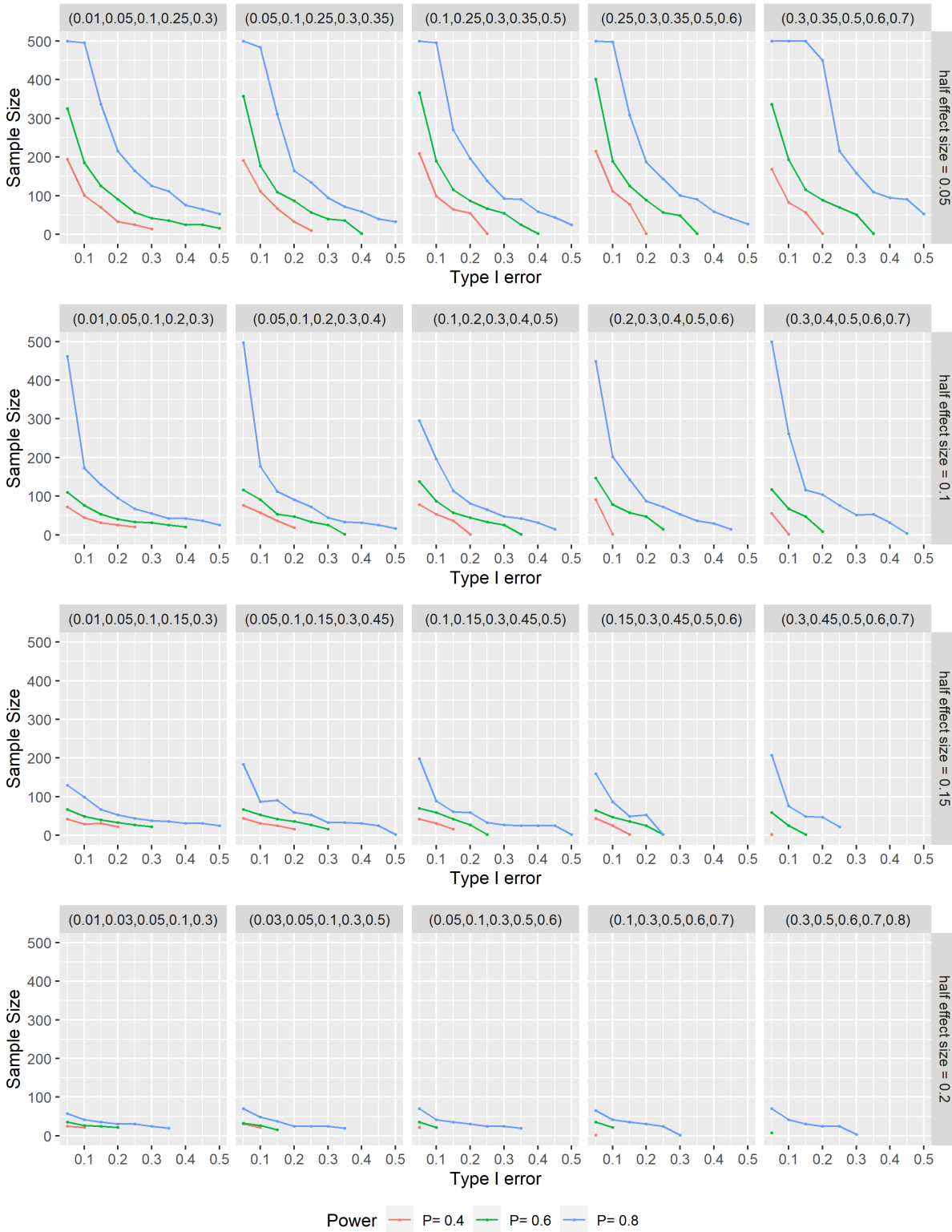


Figure A.1: Sample size calculated for each combination of effect size, p_1^* and candidate sample size when the Type I error rate ranges between 5% to 50%. Each row indexes a half effect size among $\epsilon_1 = \epsilon_2 = (0.05, 0.10, 0.15, 0.20)$ and each column indexes one of five scenarios for p_1^* , in which the true MTD locates at a different dose level. In each sub-figure, each color indexes a power among (0.4, 0.6, 0.8).

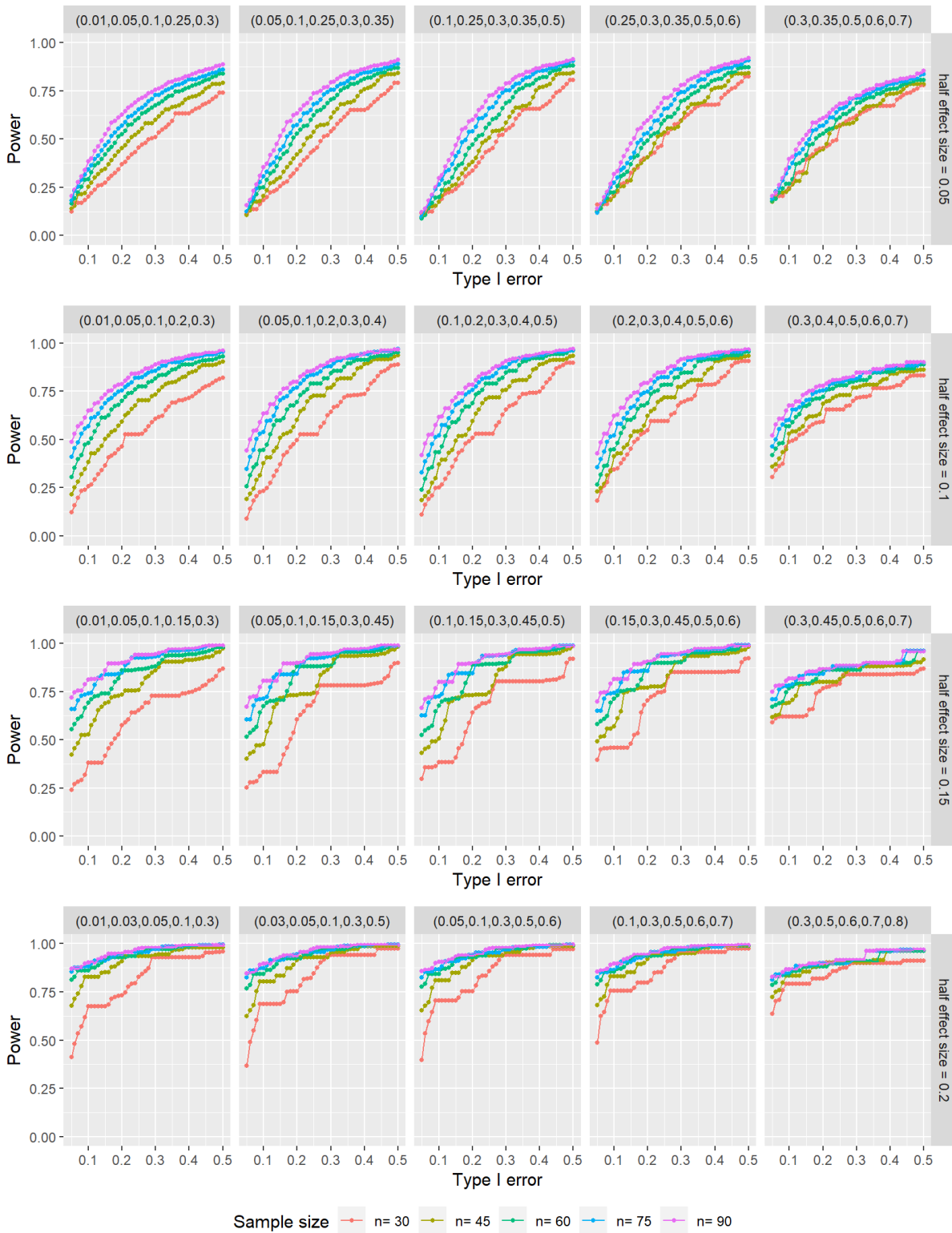


Figure A.2: Power calculated for each combination of effect size $\epsilon_1 = \epsilon_2$, \mathbf{p}_1^* and candidate sample size when the Type I error rate range between 5% to 50%. Each row indexes a half effect size among $\epsilon_1 = \epsilon_2 = (0.05, 0.10, 0.15, 0.20)$ and each column indexes one of five scenarios for \mathbf{p}_1^* , in which the true MTD locates at a different dose level. In each sub-figure, each colors indexes a candidate sample size among $n = (30, 45, 60, 75, 90)$.

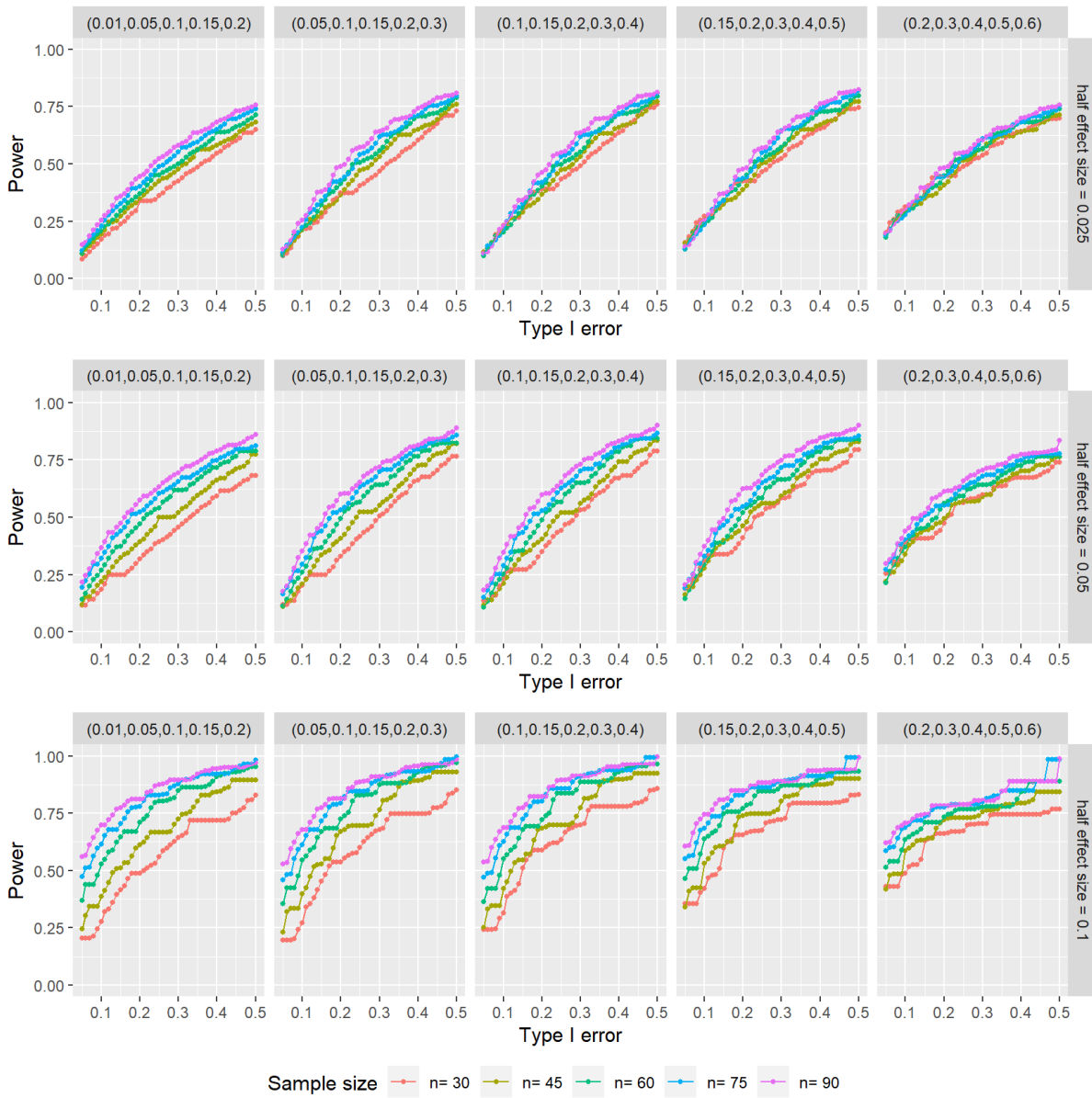


Figure B.3: Power calculated for each combination of effect size, p_1^* and candidate sample size when the Type I error rate ranges between 5% to 50%. Each row indexes a half effect size among $\epsilon_1 = \epsilon_2 = (0.05, 0.10, 0.15, 0.20)$ and each column indexes one of five scenarios for p_1^* , in which the true MTD locates at a different dose level. In each sub-figure, each color indexes a candidate sample size among $n = (30, 45, 60, 75, 90)$.

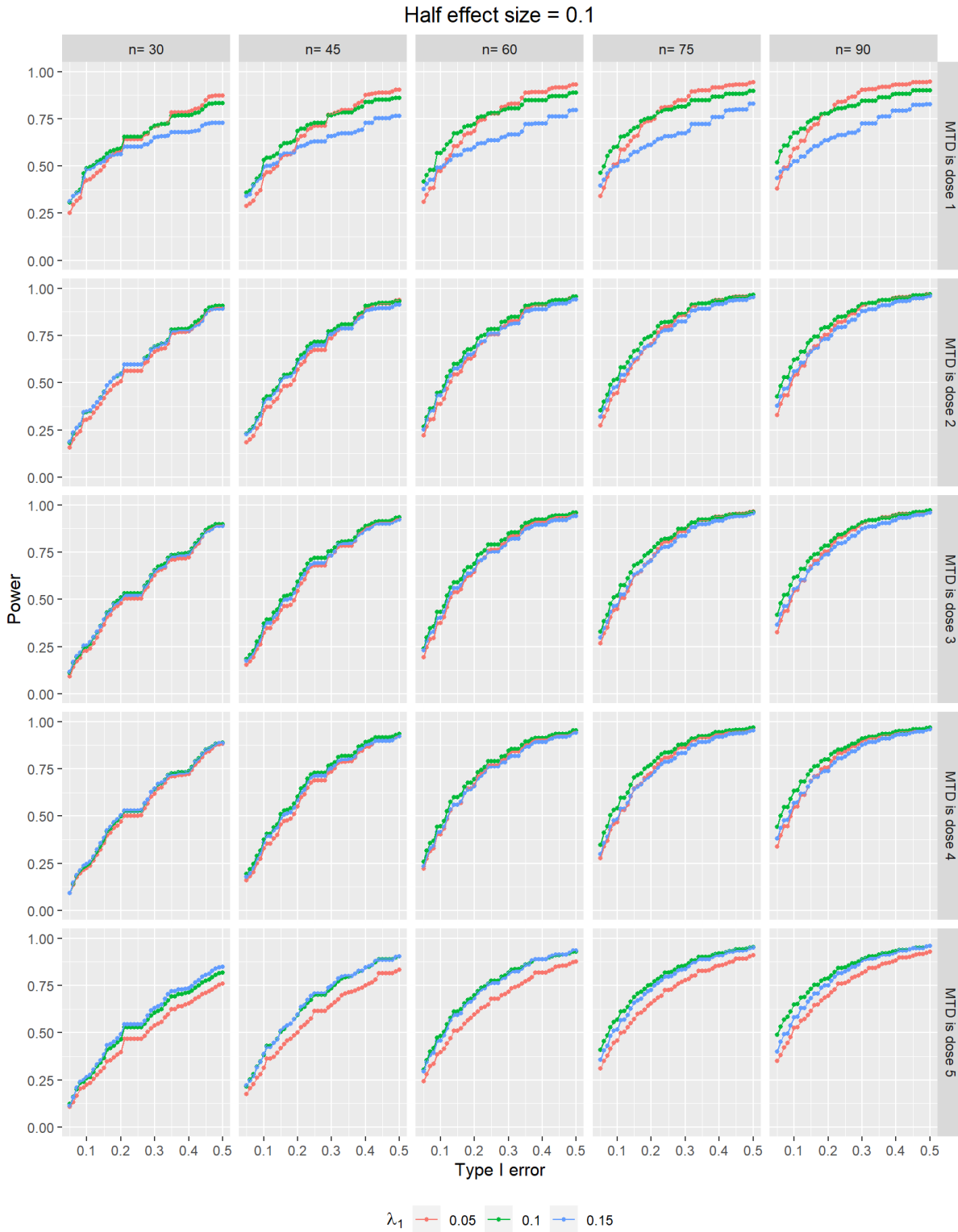


Figure C.4: Power calculated for each combination of λ_1 and candidate sample size when the Type I error rate ranges between 5% to 50% and half effect size $\epsilon_1 = \epsilon_2 = 0.1$. Each row indexes an alternative scenario for \mathbf{p}_1^* and each column indexes a candidate sample size. In each sub-figure, each color indexes a different value for λ_1 .

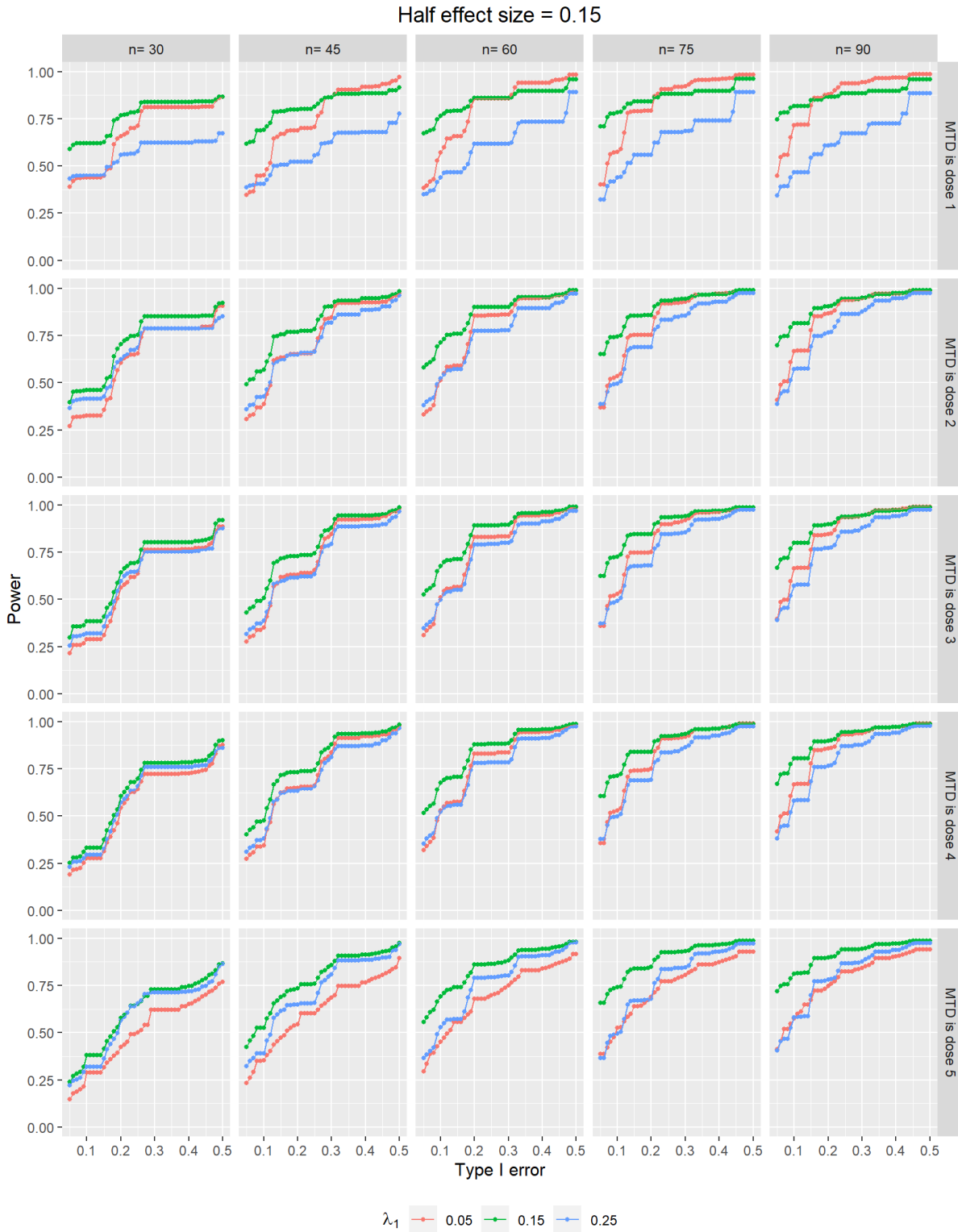


Figure C.5: Power calculated for each combination of λ_1 and candidate sample size when the Type I error rate ranges between 5% to 50% and half effect size $\epsilon_1 = \epsilon_2 = 0.15$. Each row indexes an alternative scenario for \mathbf{p}_1^* and each column indexes a candidate sample size. In each sub-figure, each color indexes a different value for λ_1 .

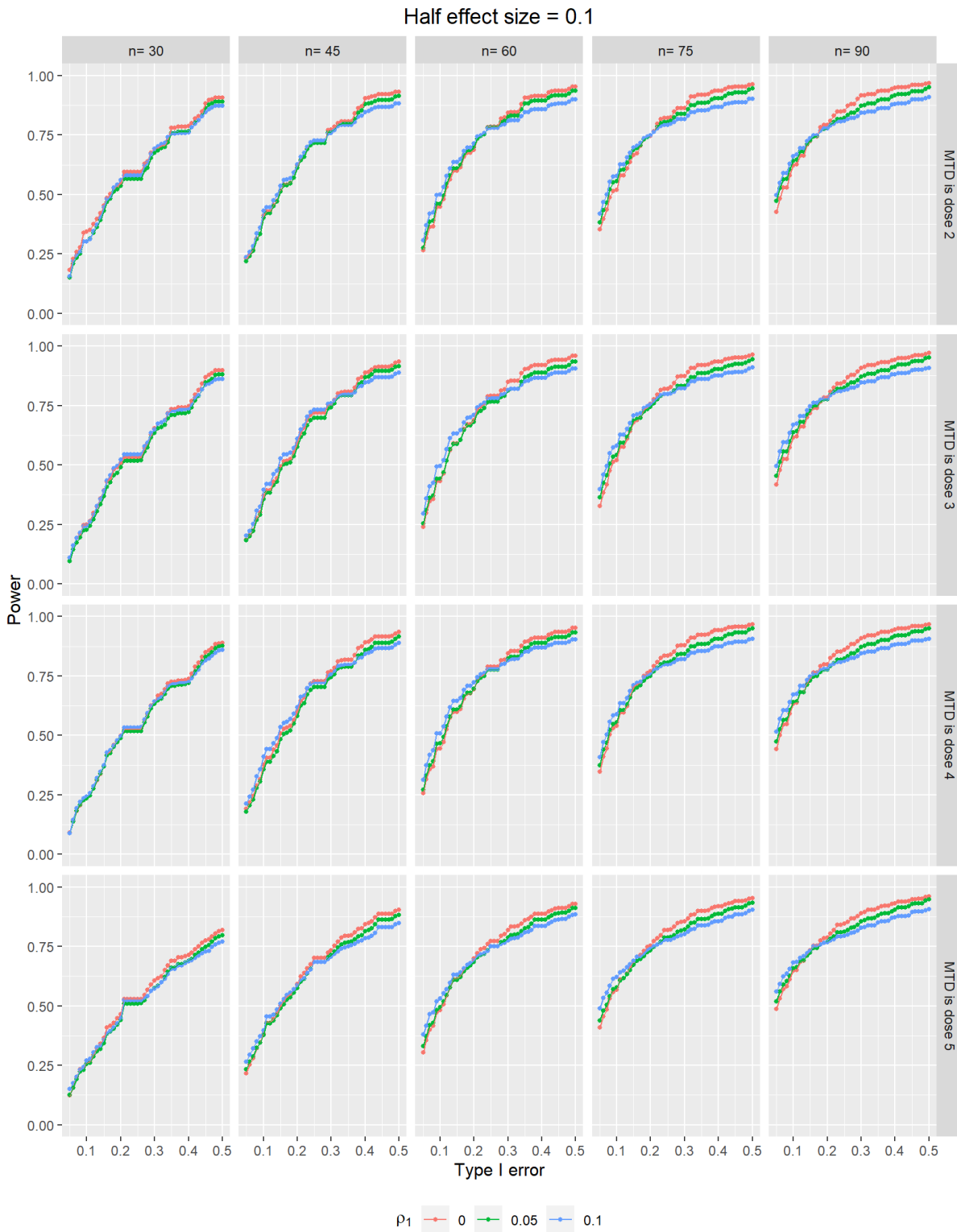


Figure C.6: Power calculated for each combination of ρ_1 and candidate sample size when the Type I error rate ranges between 5% to 50% and half effect size $\epsilon_1 = \epsilon_2 = 0.1$. Each row indexes an alternative scenario for \mathbf{p}_1^* and each column indexes a candidate sample size. In each sub-figure, each color indexes a different value for ρ_1 .

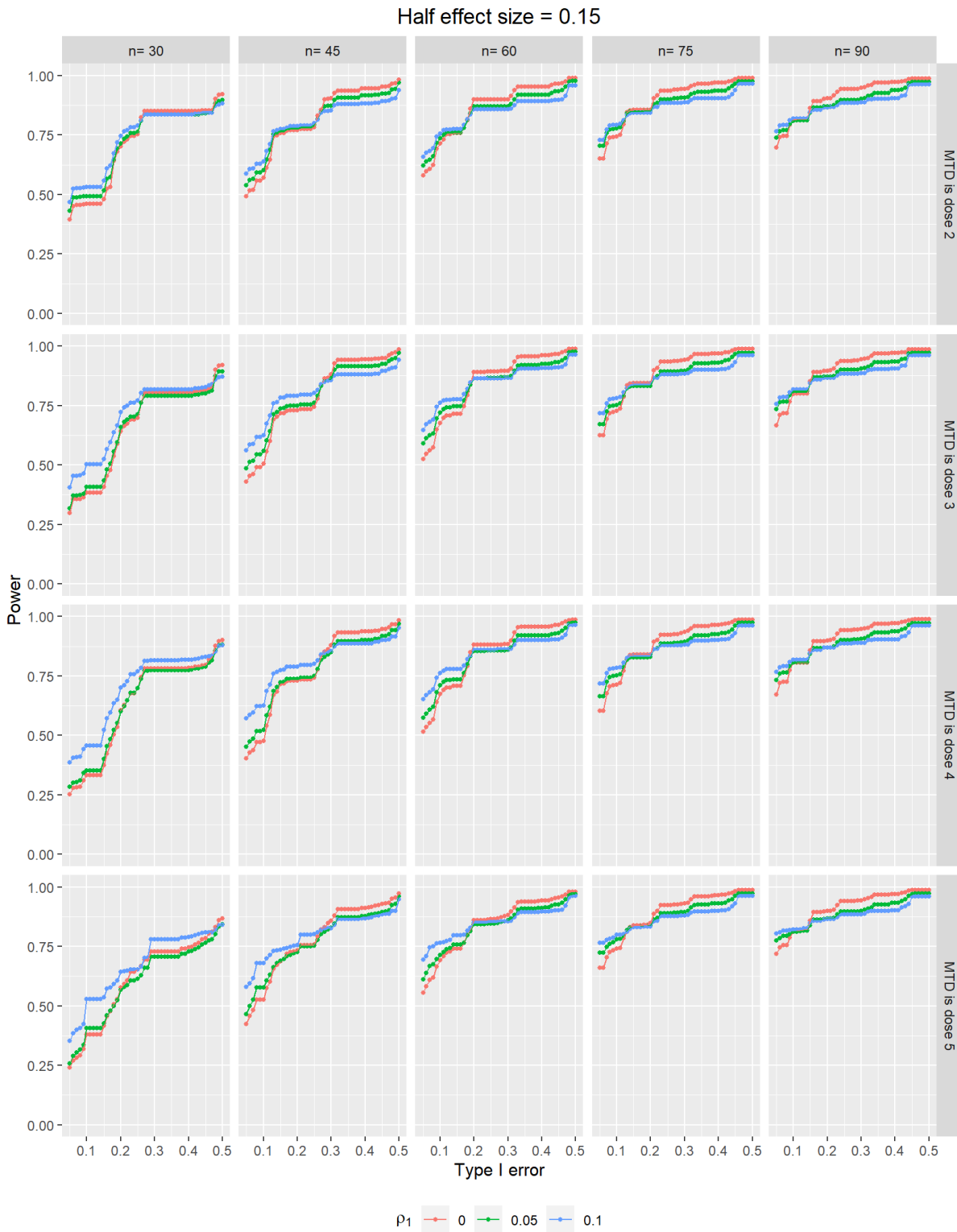


Figure C.7: Power calculated for each combination of ρ_1 and candidate sample size when the Type I error rate ranges between 5% to 50% and half effect size $\epsilon_1 = \epsilon_2 = 0.15$. Each row indexes an alternative scenario for \mathbf{p}_1^* and each column indexes a candidate sample size. In each sub-figure, each color indexes a different value for ρ_1 .

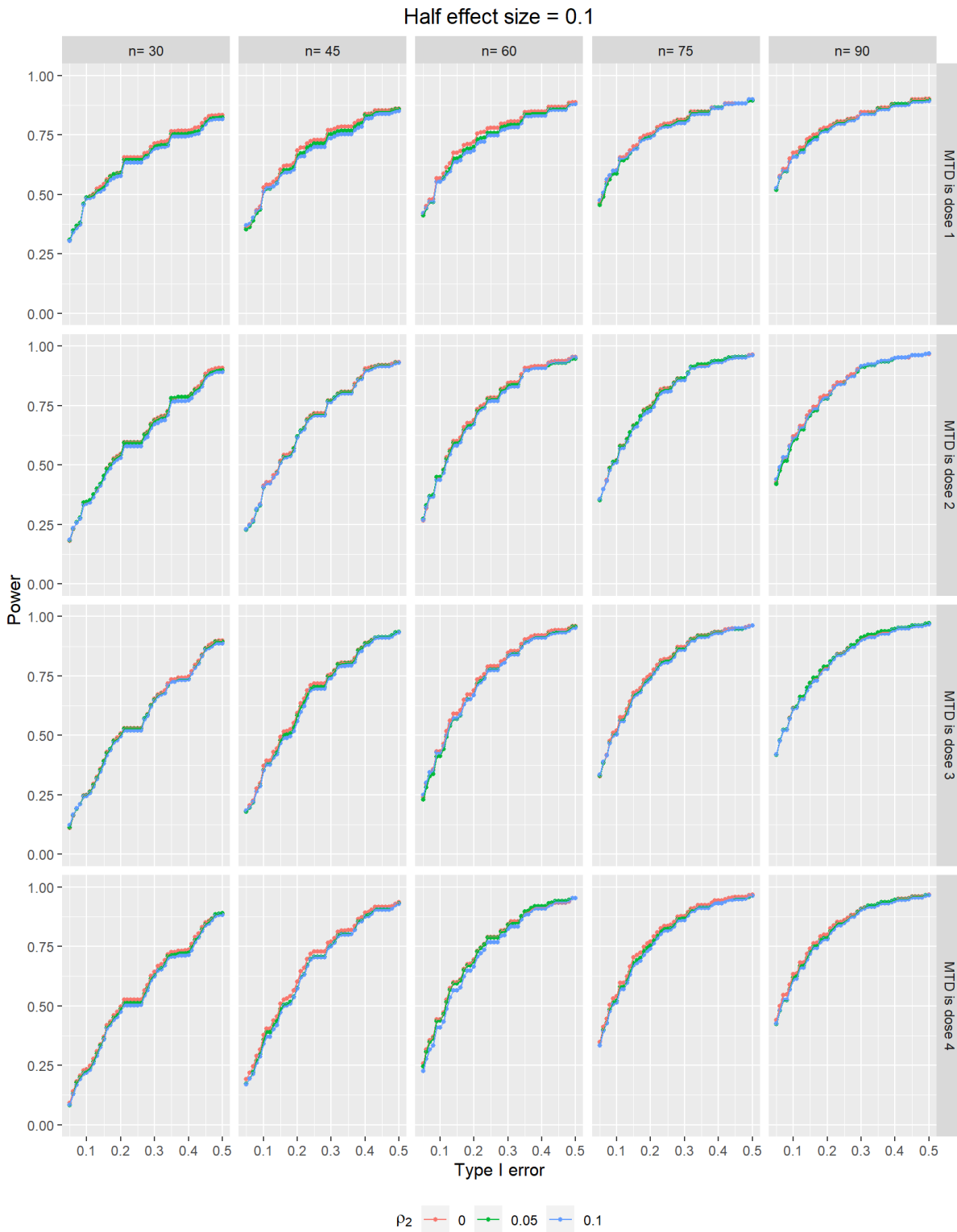


Figure C.8: Power calculated for each combination of ρ_2 and candidate sample size when the Type I error rate ranges between 5% to 50% and half effect size $\epsilon_1 = \epsilon_2 = 0.1$. Each row indexes an alternative scenario for \mathbf{p}_1^* and each column indexes a candidate sample size. In each sub-figure, each color indexes a different value for ρ_2 .

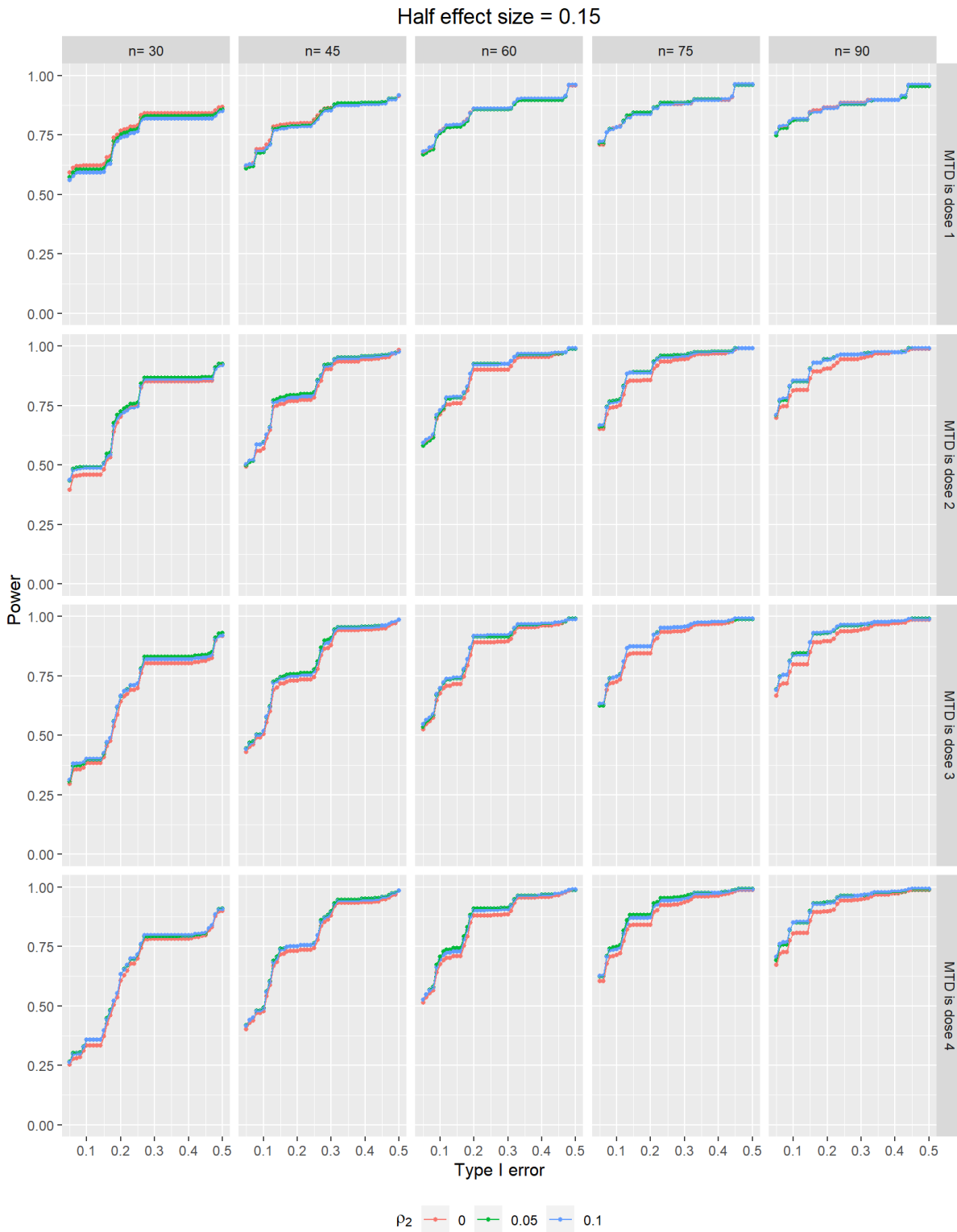


Figure C.9: Power calculated for each combination of ρ_2 and candidate sample size when the Type I error rate ranges between 5% to 50% and half effect size $\epsilon_1 = \epsilon_2 = 0.15$. Each row indexes an alternative scenario for \mathbf{p}_1^* and each column indexes a candidate sample size. In each sub-figure, each color indexes a different value for ρ_2 .

Appendix D Sensitivity analysis

D.1 A simple specification of q^{ij}

The vectors $q^{ij} = (q_1^{ij}, \dots, q_D^{ij})$ used in the fitting priors in (7) and (8) are the modes of D truncated Beta distributions under different augmented model M_{ij} , $i = 0, 1$, $j = 0, 1, \dots, D$, if $i = 0$ and $j = 1, \dots, D$, if $i = 1$, which can be simply elicited as follows:

$$q_k^{ij} = \begin{cases} a_1 * (p_T - \epsilon_1), & \text{if } i = 1, k < j - 1 \text{ or } i = 0, k < D - j \\ a_2 * (p_T - \epsilon_1), & \text{if } i = 1, k = j - 1 \text{ or } i = 0, k = D - j & k = 1, 2, \dots, D; \\ p_T, & \text{if } i = 1, k = j & j = 1, \dots, D, \text{ if } i = 1; \\ a_3 * (p_T + \epsilon_2), & \text{if } i = 1, k = j + 1 \text{ or } i = 0, k = D - j + 1 & j = 0, 1, \dots, D, \text{ if } i = 0, \\ a_4 * (p_T + \epsilon_2), & \text{if } i = 1, k > j + 1 \text{ or } i = 0, k > D - j + 1 \end{cases} \quad (\text{D.1})$$

where $0 < a_1, a_2 < 1$ and $a_3, a_4 > 1$. Note that we use $p_T - \epsilon_1$ and $p_T + \epsilon_2$ in (D.1) to force each element of the mode vector to be located within each corresponding truncated interval. Table D.1 shows an example when $D = 5$, $p_T = 0.30$, $\epsilon_1 = \epsilon_2 = 0.10$, $a_1 = 0.6$, $a_2 = 0.9$, $a_3 = 1.05$ and $a_4 = 1.2$.

Table D.1: An example of modes q^{ij} in the fitting priors

M_{ij}	M_{11}	M_{12}	M_{13}	M_{14}	M_{15}	M_{00}	M_{01}	M_{02}	M_{03}	M_{04}	M_{05}
q_k^{ij}	q^{11}	q^{12}	q^{13}	q^{14}	q^{15}	q^{00}	q^{01}	q^{02}	q^{03}	q^{04}	q^{05}
$q_1^{\cdot\cdot}$	0.30	0.18	0.12	0.12	0.12	0.12	0.12	0.12	0.12	0.18	0.42
$q_2^{\cdot\cdot}$	0.42	0.30	0.18	0.12	0.12	0.12	0.12	0.12	0.18	0.42	0.48
$q_3^{\cdot\cdot}$	0.48	0.42	0.30	0.18	0.12	0.12	0.12	0.18	0.42	0.48	0.48
$q_4^{\cdot\cdot}$	0.48	0.48	0.42	0.30	0.18	0.12	0.18	0.42	0.48	0.48	0.48
$q_5^{\cdot\cdot}$	0.48	0.48	0.48	0.42	0.30	0.18	0.42	0.48	0.48	0.48	0.48

D.2 Simulation results

For sensitivity analysis, three types of the sampling priors under H_0 (described in Section 2.4) are used, with $c = 0$ (vague prior) and $c = 48$ (informative prior). Here, the half effect size is fixed at 0.1. Results are illustrated in Figures D.10, D.11 and D.12.

Figure D.10 indicates that the specification of the sampling prior under H_0 has large impact on the sample size determination. The order statistics of the uniform distribution has the largest power among all situations, uniform with monotonicity comes second, and the point mass has the smallest power given a candidate sample size. The order statistics of the uniform distribution is the most dispersed prior across the dose range from Figure 2 and as a result, more doses are further away from p_T . Therefore, it is easier to accept H_0 when H_0 is true, and the calibrated BF_0 from step 1 is larger.

Figures D.11 and D.12 indicate that, the effects of dispersion parameter c and mode vector \mathbf{q}^{1j} and \mathbf{q}^{0j} are generally small and dependent on the sampling prior $\pi_0^{(s)}(\mathbf{p} | H_0)$ and \mathbf{p}_1^* . Here, we investigated two configurations of the mode vector: in Mode 1, we have $(a_1, a_2, a_3, a_4) = (0.6, 0.9, 1.05, 1.2)$, and in Mode 2, $(a_1, a_2, a_3, a_4) = (0.3, 0.5, 1.2, 1.5)$. When the order statistics of the uniform is used as the sampling prior under H_0 , different configurations of c , \mathbf{q}^{1j} and \mathbf{q}^{0j} give similar results. However, when the uniform with monotonicity is used as the sampling prior, the vague fitting prior when $c = 0$ provides larger power than when $c = 48$. The fitting prior with mode 1 has larger power than mode 2, which is expected due to its similarity with the \mathbf{p}_1^* scenario.

Appendix E Practical Application for $p_T = 0.2$

Table E.2: For each combination of effect size, Type I error rate and candidate sample size, the range of the power given $p_T = 0.2$ is calculated using five different scenarios for \mathbf{p}_1^* where in each scenario, the true MTD locates at each different dose level.

Half effect size	Type I error	Power range				
		n=30	n=45	n=60	n=75	n=90
0.025	0.05	0.09~0.20	0.11~0.19	0.10~0.18	0.11~0.19	0.11~0.20
	0.1	0.17~0.31	0.19~0.29	0.20~0.29	0.22~0.28	0.23~0.30
	0.2	0.34~0.45	0.35~0.41	0.37~0.45	0.40~0.45	0.44~0.49
	0.3	0.43~0.54	0.48~0.56	0.50~0.57	0.55~0.64	0.58~0.64
	0.4	0.55~0.65	0.58~0.67	0.64~0.73	0.65~0.74	0.68~0.76
	0.5	0.65~0.76	0.68~0.77	0.71~0.80	0.74~0.82	0.76~0.82
0.05	0.05	0.12~0.25	0.11~0.22	0.11~0.21	0.15~0.27	0.18~0.30
	0.1	0.19~0.39	0.21~0.34	0.25~0.37	0.29~0.40	0.35~0.44
	0.2	0.32~0.47	0.39~0.49	0.47~0.56	0.52~0.55	0.57~0.62
	0.3	0.46~0.60	0.52~0.59	0.62~0.66	0.66~0.72	0.69~0.75
	0.4	0.59~0.70	0.66~0.75	0.72~0.79	0.75~0.81	0.77~0.85
	0.5	0.68~0.79	0.76~0.84	0.77~0.84	0.78~0.87	0.84~0.90
0.1	0.05	0.20~0.43	0.23~0.42	0.36~0.52	0.46~0.59	0.53~0.62
	0.1	0.27~0.49	0.39~0.58	0.53~0.64	0.61~0.69	0.68~0.74
	0.2	0.49~0.66	0.61~0.74	0.71~0.77	0.78~0.83	0.78~0.85
	0.3	0.64~0.72	0.72~0.80	0.78~0.88	0.80~0.91	0.81~0.91
	0.4	0.72~0.79	0.79~0.90	0.84~0.93	0.85~0.94	0.89~0.96
	0.5	0.77~0.86	0.84~0.93	0.89~0.97	0.98~1.00	0.97~1.00

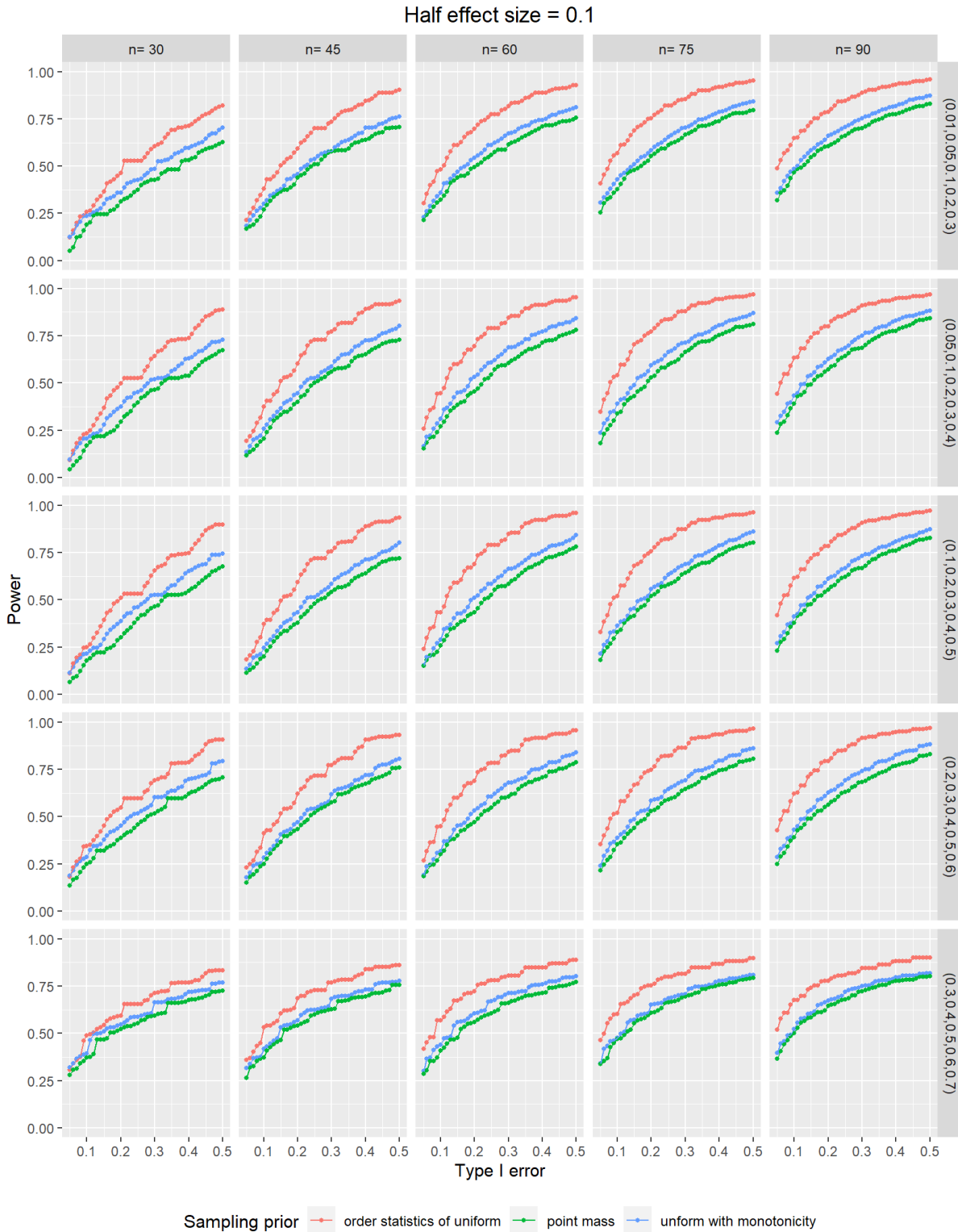


Figure D.10: Power calculated for each combination of \mathbf{p}_1^* and candidate sample size when the Type I error rate ranges between 5% to 50% and half effect size $\epsilon_1 = \epsilon_2 = 0.1$. Each row indexes an alternative scenario for \mathbf{p}_1^* and each column indexes a candidate sample size. In each sub-figure, each color indexes a different configuration for $\pi_0^{(s)}(\mathbf{p} | H_0)$.

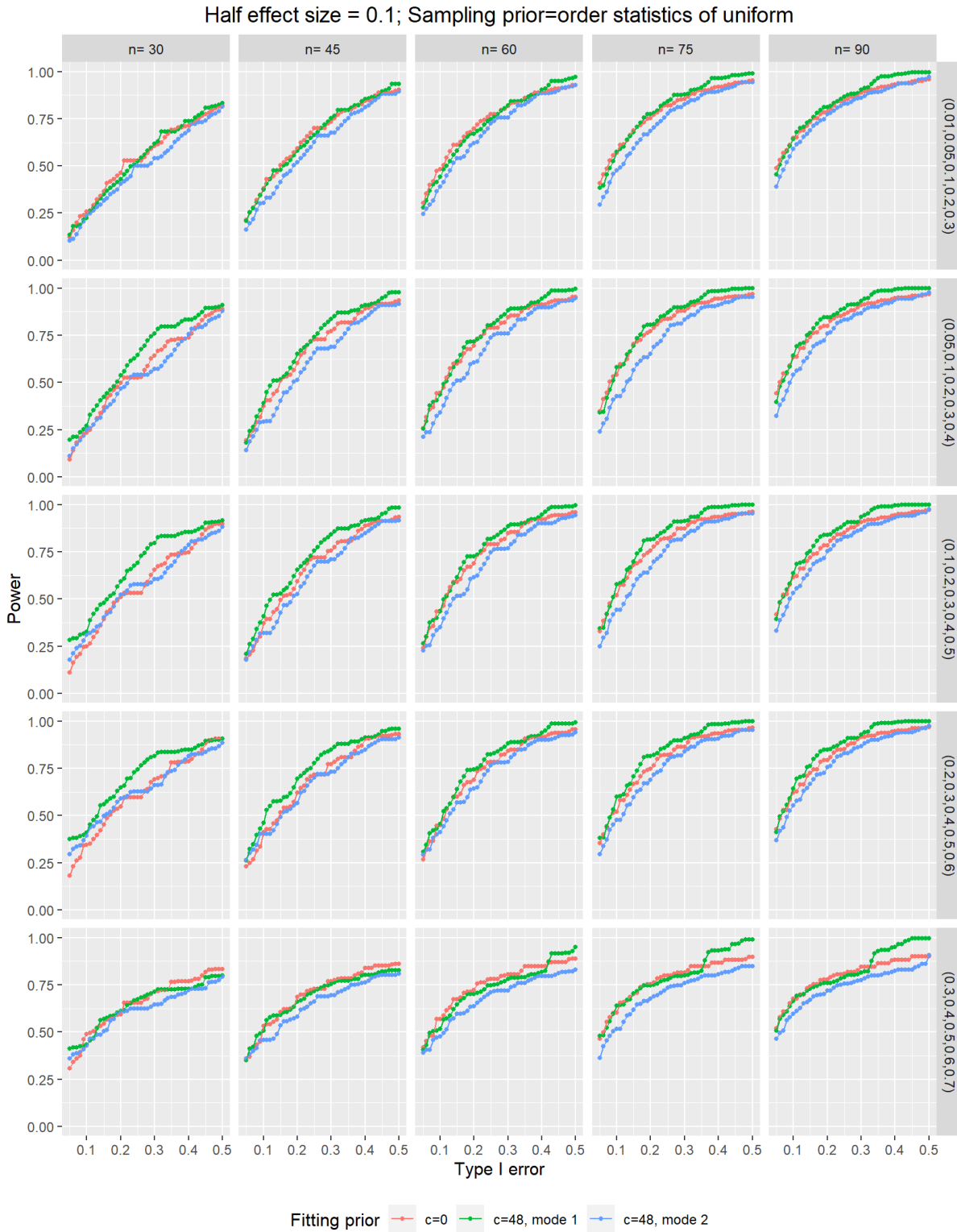


Figure D.11: Power calculated for each combination of \mathbf{p}_1^* and candidate sample size when the Type I error rate ranges between 5% to 50%, half effect size $\epsilon_1 = \epsilon_2 = 0.1$ and $\pi_0^{(s)}(\mathbf{p} | H_0)$ fixed. Each row indexes an alternative scenario for \mathbf{p}_1^* and each column indexes a candidate sample size. In each sub-figure, each color indexes a different configuration for c , \mathbf{q}^{1j} and \mathbf{q}^{0j} .

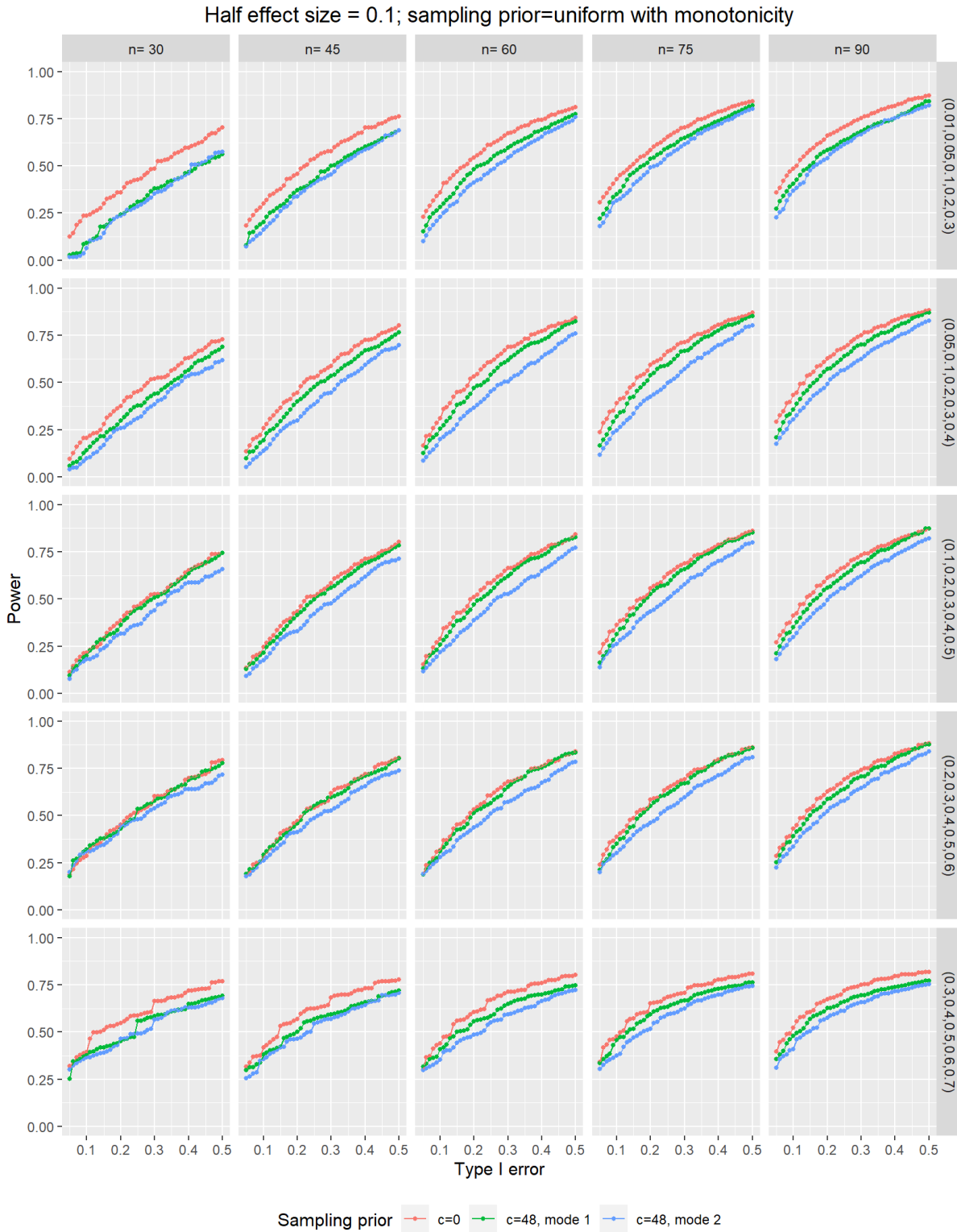


Figure D.12: Power calculated for each combination of \mathbf{p}_1^* and candidate sample size when the Type I error rate ranges between 5% to 50%, half effect size $\epsilon_1 = \epsilon_2 = 0.1$ and $\pi_0^{(s)}(\mathbf{p} | H_0)$ fixed. Each row indexes an alternative scenario for \mathbf{p}_1^* and each column indexes a candidate sample size. In each sub-figure, each color indexes a different configuration for c , \mathbf{q}^{1j} and \mathbf{q}^{0j} .